1987

Vacuum Growth and Characterization of Thin Films of Zinc Tin Diphosphide.

Hyun Yong Shin
Louisiana State University and Agricultural & Mechanical College

INFORMATION TO USERS

While the most advanced technology has been used to photograph and reproduce this manuscript, the quality of the reproduction is heavily dependent upon the quality of the material submitted. For example:

- Manuscript pages may have indistinct print. In such cases, the best available copy has been filmed.

- Manuscripts may not always be complete. In such cases, a note will indicate that it is not possible to obtain missing pages.

- Copyrighted material may have been removed from the manuscript. In such cases, a note will indicate the deletion.

Oversize materials (e.g., maps, drawings, and charts) are photographed by sectioning the original, beginning at the upper left-hand corner and continuing from left to right in equal sections with small overlaps. Each oversize page is also filmed as one exposure and is available, for an additional charge, as a standard 35mm slide or as a 17"x 23" black and white photographic print.

Most photographs reproduce acceptably on positive microfilm or microfiche but lack the clarity on xerographic copies made from the microfilm. For an additional charge, 35mm slides of 6"x 9" black and white photographic prints are available for any photographs or illustrations that cannot be reproduced satisfactorily by xerography.

Order Number 8728216

Vacuum growth and characterization of thin films of zinc tin diphosphide

Shin, Hyun Yong, Ph.D.

The Louisiana State University and Agricultural and Mechanical Col., 1987

U·M·I
300 N. Zeeb Rd.
Ann Arbor, MI 48106

VACUUM GROWTH AND CHARACTERIZATION OF THIN FILMS OF ZINC TIN DIPHOSPHIDE

A Dissertation

Submitted to the Graduate Faculty of the
Louisiana State University and
Agricultural and Mechanical College
in partial fulfillment of the
requirements for the degree of
Doctor of Philosophy

in

The Department of
Electrical and Computer Engineering

by
Hyun Yong Shin
B.S., Yonsei University, 1979
M.E., Yonsei University, 1981
August 1987

ACKNOWLEDGEMENTS

I wish to express my gratitude to Dr. Pratul K. Ajmera for his continued guidance, assistance, encouragement, and friendship during my graduate program. I would like to thank to Dr. Subhash C. Kak and Dr. Burke Huner for their friendship and some helpful discussions, to Dr. H.S. Ullal of Solar Energy Research Institute for providing the AES and WDS analyses on some samples, to Dr. S.F. Watkins of Chemistry Department at LSU for useful discussions on X-Ray diffraction data, and to Dr H.C. Eaton and Dr. R.E. Ferrell for their assistance in the use of SEM and X-Ray diffraction instruments. Appreciation is also expressed to Dr. Jesse M. Janes who allowed the author use of his computer and printer in preparing this dissertation.

I especially thank to God for giving me a good opportunity to study at Louisiana State University.

I am grateful to my wife, Shin-Hwa, for her understanding, unquestioned support, and encouragement during the years in graduate school. The love and joy we share with each other and with my children, Emily and Peter, makes this exsistence tolerable.

I express thanks to other faculty members and graduate students for friendship, association, and assistance during

the years of research reported in this dissertation.

The research reported herein was supported in part by the National Science Foundation through the Engineering Research Equipment Grant and mostly by Solar Energy Research Institute through Subcontract No. XL-4-03032-2 and their support is sincerely appreciated.

TABLE OF CONTENTS

TABLE OF CONTENTS (cont'd)

LIST OF TABLES

LIST OF TABLES (cont'd)

LIST OF FIGURES

LIST OF FIGURES (cont'd)

LIST OF FIGURES (cont'd)

LIST OF FIGURE (cont'd)

ABSTRACT

A vacuum growth technique has been employed for the first time to grow thin films of $ZnSnP_2$. Near stoichiometric thin films of polycrystalline $ZnSnP_2$ have been grown on GaAs and quartz substrates. A reasonable degree of reproducibility of the film composition from one run to the next was achieved by using a quadrupole mass analyzer probe in conjunction with a digital feedback controller to maintain constant Zn flux. The growth parameters for the system including the estimates for the Zn/Sn flux ratio at the substrate and the optimum substrate temperature have been obtained for the near stoichiometric film growth. The most uniform films showed less than ±0.75% variation in the atomic composition for each of the three elements across a 1 cm^2 sample.

The quality of layers grown on GaAs substrates was superior to those on quartz substrates. Different analytical techniques were used to characterize the grown films. The relations between film surface morphology and film composition were obtained from SEM and EDS analyses. The film morphology was most sensitive to the Zn content in the film. An absorption coefficient of greater than 10^5 cm^{-1} was obtained without taking surface scattering into

account. The energy gap value of 1.62 eV was observed from the optical transmission analysis. X-Ray diffraction analysis indicated that the grown films have chalcopyrite structure with lattice constant values in the range of 5.64-5.67 Å. Silver and Indium were used to form electrical contacts to the grown films. Resistivity and Hall measurements were made in the temperature range of 300-625°K. All the films examined were of p-type conductivity and the film resistivity was in the range of 0.1-10 Ω-cm. The carrier concentrations in these p-type films were in the range of 10^{16}-10^{18} cm^{-3} and the room temperature Hall mobility values were in the range of 35-47 cm^2/V-sec. A small decrease in the bulk resistivity value was observed at 77°K. Heterostructure diodes fabricated from the p-type $ZnSnP_2$ films grown on n-type GaAs substrates showed a small photoresponse demonstrating the feasibility of photovoltaic application of the grown material.

CHAPTER 1

INTRODUCTION

Early work on semiconducting materials concentrated on group IV elemental semiconductors such as Ge and Si. Later, semiconducting binary compounds were formed by replacing group IV elements by atoms of the adjacent III and V groups resulting in diamond-like structure(covalent bonding and tetrahedral atomic arrangement) found in group IV elemental semiconductors. It was realized, in the mid fifties, that just as these binary compounds resulted from the heterovalent substitution of group IV elements, there should also exist a group of ternary semiconducting compounds producible in a similar way by replacing one of the atoms of a binary compound. Following the confirmation of the existence of such ternary semiconducting compounds, a respectable amount of work has been done on them; including those of the II-IV-V_2 type, in which the group III atoms of the III-V compounds are substituted by the group II and the group IV atoms.

A number of ternary semiconducting compounds of the form II-IV-V_2 such as $CdGeP_2$, $ZnSiP_2$ and $ZnSnP_2$ have so far been found. These materials usually crystallize in the chalcopyrite structure. Interest in these materials has remained high because of their many interesting potential applications. The wide range of energy gaps available from

0.26 eV for $CdSnAs_2$ to 3.06 eV for $ZnSiP_2$ along with their interesting optical properties make these analogs of the binary III-V compound semiconductors important for various optical and electro-optic applications [1,2]. The information on ternary II-IV-V_2 semiconductor material properties show that these materials can be useful in various applications such as microwave devices, optical devices, light sources and photodetectors [3-8].

1.1 Growth Techniques for II-IV-V_2 Compound Semiconductors

Many techniques have been employed for the growth of ternary II-IV-V_2 compound semiconductor materials. Important among them are direct melt growth, dilute solution growth, chemical vapor deposition, and liquid phase epitaxial growth. Each of these growth techniques is briefly reviewed here.

1.1.1 Direct Melt Growth

Direct melt growth is the direct synthesis of compound semiconductors from the constituent elements by gradual heating of the stoichiometric mixture, subsequent melting, followed by slow cooling through the freezing point of the desired material. This technique yields large crystals and is preferred if the dissociation pressure is relatively low and controllable. Direct melt growth technique includes Bridgman, zone melting, and horizontal directional

solidification techniques [9,10]. All of the ternary II-IV-V_2 arsenides except $CdSiAs_2$ which decomposes at about 850°C have been synthesized by this technique. Some of the ternary II-IV-V_2 phosphides such as $CdGeP_2$, $ZnGeP_2$, and $ZnSiP_2$ have been grown by direct melting of the II-V_2 phosphides with the group IV elements [1,11,12].

1.1.2 Dilute Solution Growth

Dilute solution growth technique has been widely utilized especially for the compounds which cannot be prepared by direct melt growth from stoichiometric mixture of elements due to their high dissociation pressure at the melting point. Sn, Bi, Sb and Tl are often used as solvents [11,13,14]. Stoichiometric amounts of constituent elements with sufficient amount of solvent to make few mole percent solution of ternary compound are placed in a suitable crucible and then sealed in an evacuated thick-walled quartz ampoule. This ampoule is heated to and held at the desired temperature in the furnace and then slowly cooled. This growth technique generally produces small crystals because of the random direction of nucleation. The slow cooling rate is the most critical parameter that controls the quality of the grown crystals. The morphology of the resulting crystals is often platelets or needle-like. All of the ternary II-IV-V_2 phosphides and some of II-IV-V_2 arsenides such as $ZnSiAs_2$ and $ZnSnAs_2$ have been grown by the

dilute solution growth technique. Excessive residual solvent such as Sn is removed from the grown crystals with reactants such as hot, concentrated HCl or by dissolving in heated Hg. $ZnSnP_2$ has been grown from dilute solutions of Zn and P in Sn melt [1] and from dilute solution of ZnP_2 in Sn melt [15].

1.1.3 Chemical Vapor Deposition

Chemical Vapor Deposition (CVD) utilizes the chemical transport reaction for crystallization from the constituents in the vapor phase. This technique with closed tube method has been applied for preparing ternary II-IV-V_2 phosphides based on Si and Ge such as $ZnSiP_2$ and $CdGeP_2$ [16-18]. Frequently binary II-V_2 compounds have been prepared and used as the sources of group II and group V constituents while group IV elemenal single crystals in excess of the stoichiometric amounts have been used as sources for the group IV elements. Binary II-V_2 compound and crystals of the group IV element are respectively placed at the cold-end and the hot-end of a thick-walled quartz tube in a tilted furnace. The transport agents can be added either in the elementary form such as I_2 and Cl_2 or as compounds such as $ZnCl_2$, ZnI_2, $CdCl_2$, etc. It normally takes 5 to 10 days or more to obtain a few mm^3 size crystals. However, the attempts to grow ternary II-IV-V_2 compounds with Sn as the group III element by closed tube CVD have so far been

unsuccessful.

Metal-organic chemical vapor deposition(MOCVD) and open tube CVD techniques have been applied to grow the ternary $ZnSiAs_2$ [19,20]. Thin films of $ZnSnP_2$ has been obtained from the combined CVD/thermal ion exchange method by annealing SnO_2 thin film layers coated on the glass substrate in an ambient containing PH_3, H_2, and Zn-metal vapor [21,22]. The reported optimum annealing temperature and time were 425°C and 4.5 hours to obtain $ZnSnP_2$ films of about 0.6 μm thickness [21,22]. Recently $ZnSnP_2$ films have been deposited by MOCVD utilizing Diethylzinc(DEZ), Tetraethyltin(TESn) and PH_3 at Solar Energy Research Institute [23].

1.1.4 Liquid Phase Epitaxial Growth

Application of Liquid Phase Epitaxy (LPE) technique to the growth of thin epitaxial layers of ternary compound semiconductors on the single crystal substrates for the device applications have been extensively studied in the last decade. The LPE technique of growing epitaxial layers of ternary compound semiconductors is similar to the dilute solution growth of ternary compound semiconductors becaues the LPE technique requires the use of metal solvent. In most cases Sn has been used as a solvent to make a dilute solution of ternary compound inside a vacuum sealed quartz tube. Much of the reported LPE growth has been performed in

a closed tube by placing single crystal substrate inside the tube on a specially shaped substrate holder [24]. Epitaxial layers of many of the ternary II-IV-V_2 semiconductors such as $CdSnP_2$ and $ZnSnAs_2$ have been successfully grown on a variety of substrates [21,24-27].

Recently, liquid phase epitaxial growth in open tube system with purified hydrogen environment has been extensively applied for the preparation of high quality layers of III-V binary compound semiconductors. In principle this open tube LPE technique can also be applied for the growth of the ternary II-IV-V_2 compounds if the operating temperatures are relatively low. This requirement is to minimize the loses of the more volatile components (mainly As and P) from the melt and to prevent any dissociations of the grown layers. Such conditions can be met with proper selection of solvents and some of the ternary II-IV-V_2 compound epitaxial layers such as $ZnSnP_2$ and $ZnSnAs_2$ have been obtained on various single crystal substrates [28,29].

1.1.5 Other Growth Methods

Other techniques such as vacuum evaporation from single and multiple sources, Molecular Beam Epitaxy, sputtering, and spray pyrolysis have been employed to produce thin films of $CuInSe_2$, one of the ternary I-III-VI_2 compound semiconductors [30-32]. However, very little work has been

reported for the growth of ternary II-IV-V_2 compound semiconductors by some of the above techniques.

RF sputtering has been used to produce thin films of $CdSiAs_2$ from the targets of cold-pressed and annealed $CdAs_2$ discs onto single crystal Si wafers of sizes larger than the $CdAs_2$ disc [33]. Thin films of amorphous and single crystal $ZnGeAs_2$ have been obtained using RF sputtering technique from the polycrystalline $ZnGeAs_2$ wafer targets [34] sliced from a ingot grown by a modified Bridgman technique [10]. Molecular beam epitaxy growth technique has been tried to deposit thin films of $CdSnP_2$ on single crystal InP [35]. The quality of $CdSnP_2$ layers obtained was polycrystalline and no further work has been reported on MBE growth of $CdSnP_2$ films. No work has so far been reported on vacuum growth of thin films of $ZnSnP_2$, even though some encouraging result have been obtained from the initial attempts made in this regard on our laboratory [36].

1.2 Objectives

$ZnSnP_2$ is a relatively little studied semiconductor and a member of the II-IV-V_2 group compounds. It is the direct ternary analog of III-V binary compounds GaP and InP and crystallizes either in the chalcopyrite structure or in the disordered sphalerite structure. Its unit cell containing 16 atoms in the chalcopyrite case as shown schematically in Figure 1.1. The chalcopyrite structure consists of unit

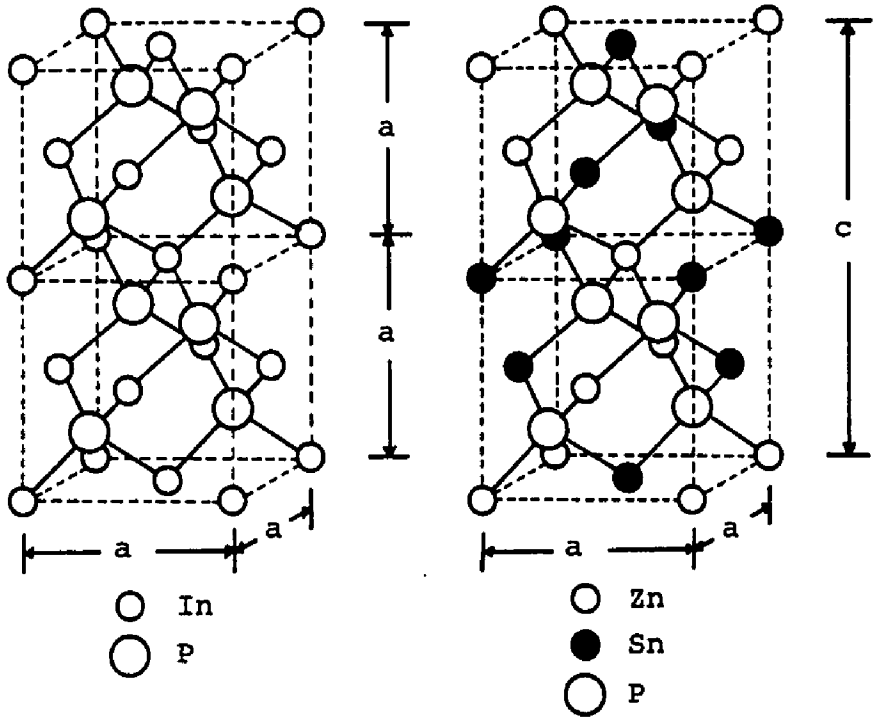

Figure 1.1 Comparision of Zinc Blende InP and Chalcopyrite $ZnSnP_2$

cells in which each cation is tetrahedrally bonded to each of two different anions. The lattice constants values of $ZnSnP_2$ are a = 5.651 Å and c = 11.302 Å [1] with the lattice constant a value providing a good lattice match with GaAs.

The interesting point is the similarity between the structures of GaAs, a III-V binary compound, and $ZnSnP_2$. The lattice constant mismatch between $ZnSnP_2$ and GaAs is quite small being approximately 0.04%. Moreover, $ZnSnP_2$ has no tetragonal distortion with c/a = 2.0 so the c to 2a mismatch is the same as the a to a mismatch. This provides the three possible chalcopyrite orientations on a (100) GaAs substrate as illustrated in Figure 1.2. It is also of interest to know that the dilute solution-grown platelets of $ZnSnP_2$ exhibit chalcopyrite and disordered sphalerite structures having the same value for the lattice constant [1,37].

$ZnSnP_2$ has a direct energy gap of 1.66 eV which makes it attractive for photovoltaic applications [1,38]. $ZnSnP_2$ has been traditionally grown by the conventional growth methods of slow cooling of dilute solutions of Zn and P [1] or ZnP_2 [15] in a Sn melt. This technique of material preparation is slow and rather cumbersome. Moreover, the above methods do not result in the growth of the material in thin film form desirable for many applications including the case for large area photovoltaic purposes.

As reviewed in the previous section, thin films of

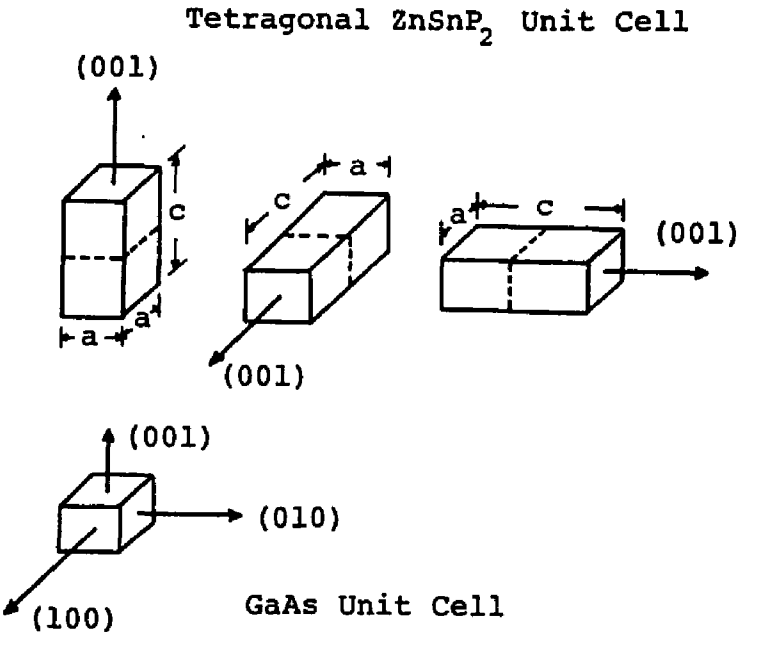

Figure 1.2 Three Possible Chalcopyrite Orientations of $ZnSnP_2$ on a (100) GaAs Substrate

$ZnSnP_2$ have been obtained by other techniques [21,28]. In the case of the combined CVD/thermal ion exchange method, gasous reactants and the products must diffuse through the entire film thickness which may result in porous or non-stoichiometric film especially if the film thickness is large. The LPE growth method is a relatively high temperature process which is, in general, not suitable for film growth on inexpensive glass substrates. Even though vacuum growth and MBE growth of thin films of some other chalcopyrite materials such as $CuInSe_2$, one of $I\text{-}III\text{-}VI_2$ group compounds, and $CdSnP_2$ have been reported [30-32,35,39], to our knowledge, no similar work, other than the one carried in our laboratory here at LSU, has been reported on the vacuum growth of thin films of $ZnSnP_2$.

This research investigates the growth of thin films of ternary chalcopyrite $ZnSnP_2$ on low cost quartz and single crystal GaAs substrates by a vacuum growth technique somewhat similar to the MBE growth process. The object of this work is to obtain the optimized growth parameters for vacuum deposition of thin films of $ZnSnP_2$ from three elemental sources and to characterize the grown films by physical, chemical, optical, and electrical analyses.

CHAPTER 2

EXPERIMENTAL

2.1 System Description

The system utilized for the growth of thin films of $ZnSnP_2$ is somewhat similar to a Molecular Beam Epitaxy (MBE) system used for the growth of compound semiconductors. Figure 2.1 shows the schematic diagram of the vacuum growth system. It consists of a vacuum system and a film growth chamber.

The growth chamber is a rectangular stainless steel box, 16" high x 12" wide x 12" deep, with hollow walls through which water can be circulated. A hinged stainless steel door sealed with Viton O-ring is used to provide an access to the inside of the growth chamber. Hot water is circulated to partially bake the chamber prior to the film growth, while cold water is circulated during the film growth to minimize the outgassing from the chamber walls. The growth chamber has provisions for a variety of electrical, optical and mechanical feedthroughs.

The primary means of achieving High Vacuum is a three stage 6 inch diameter oil diffusion pump, backed by a Welch Scientific Model 1397 mechanical rotary roughing pump. To prevent oil contamination of the growth chamber, the oil diffusion pump is equipped with a water cooled trap and a liquid nitrogen cryotrap. In addition, an oil filter is

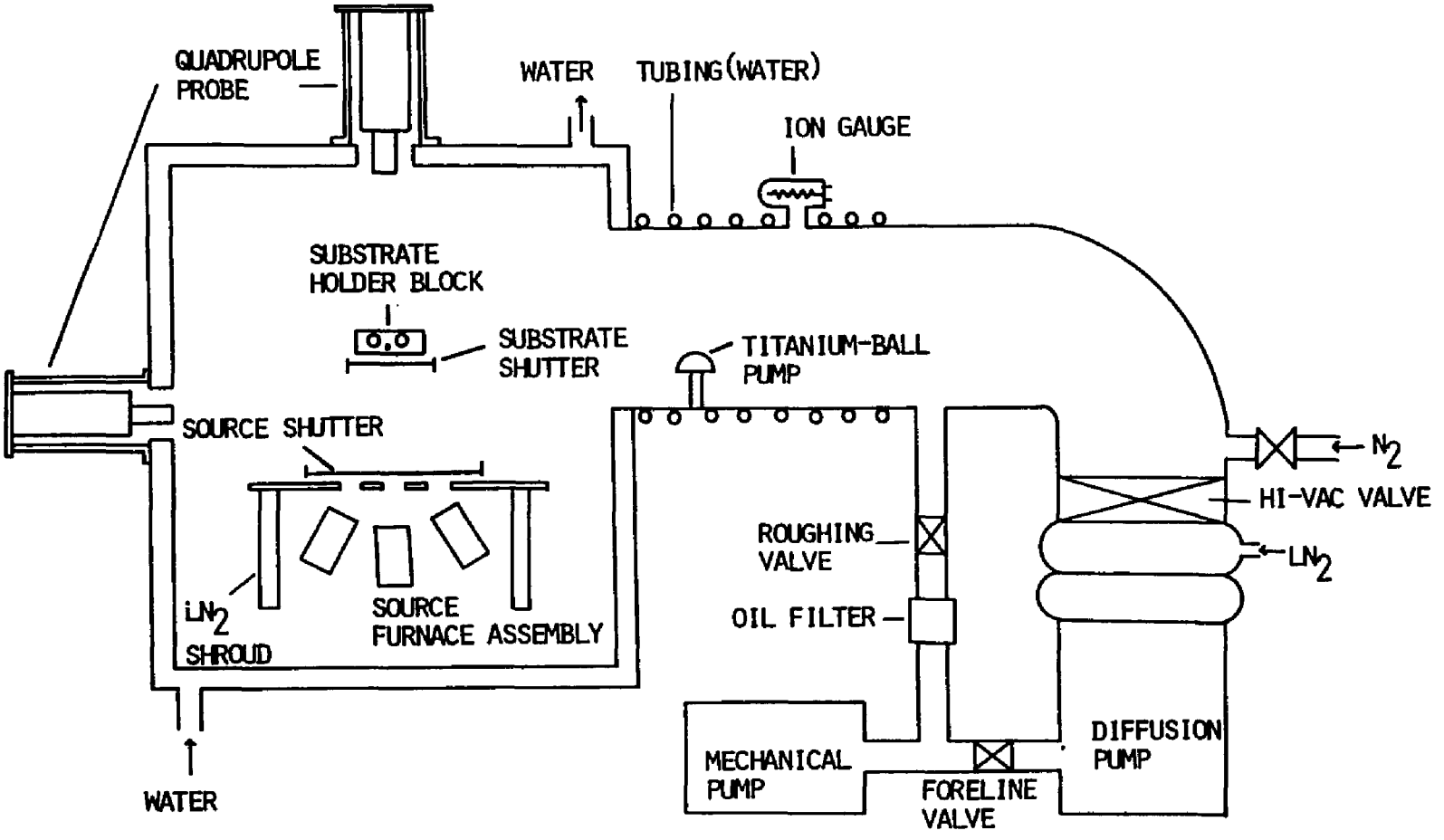

Figure 2.1 Schematic Diagram of the Vacuum Growth System

placed between the rotary roughing pump and the growth chamber to reduce oil contamination during the initial rough pumping operation. A Varian Mini-Ti-Ball sublimation pump located just behind the growth chamber inside the diffusion pump inlet provides further pumping through the chemical reactions between the sublimated titanium and the vapor species. The sublimated titanium condensed on the interior surface cooled by cold water circulation around the Ti-Ball forms a gettering surface to free the chamber from reactive gas species. A UTI Model 100C precision quadrupole mass analyzer probe is attached to the top of the chamber directly above the substrate holder block to monitor residual gas and vacuum condition. Later this probe was moved to the side of the chamber and an AMETEK/Dycor Electronics Model M200M quadrupole mass analyzer probe was attached to the top of the chamber to check and monitor Zn flux for control purposes. Details on this change will be described in Section 2.4. An ion gauge is located in the diffusion pump inlet above the Ti-Ball source.

The film growth system consists primarily of three cylindrical furnace assemblies and a substrate holder block. Each furnace assembly contains a graphite source boat for one of the three elements used in this work. The system is designed to accomodate five source furnaces. At the present time three furnaces are in use and two more can be added when required. Each furnace consists of two 2" long alumina

cylinders of diameters sized so that one fits snugly inside the other. The inner alumina cylinder is threaded and wound with annealed tantalum wire 15 mil in diameter. A graphite source boat, 1.5" long with 0.5" outside diameter and 3/8" inside diameter, is lowered from the top of the furnace and rests on the thermocouple junction. Together, this assembly is mounted on a cylindrical graphite base. The details of the furnace assembly are shown in Figure 2.2. Each furnace is shieled with a cylindrical wrap made of 5 mil thick tantalum foil 1.25" in diameter and 2.5" high.

The source furnaces are mounted on a stainless steel ring of 6.5" diameter held 2.5" above the chamber floor at an angle of 28° from the vertical so that their central axes point directly to the substrate center as shown in Figure 2.3. A molybdenum block is used as the substrate holder and is suspended above the center of the ring. The substrate holder block is heated by two imbedded Hotwatt Superwatt cartridge heaters which traverse their entire length. The furnace assemblies are enclosed by a liquid nitrogen cooled shroud. The source furnace assemblies and the substrate holder block arrangement together with the liquid nitrogen shroud are shown in Figure 2.4. A collimator plate with appropriate holes is mounted on top of the cooling shroud to direct respective fluxes to the substrate. Three stainless steel partitions are mounted to the underside of the collimator plate to isolate each source furnace assembly

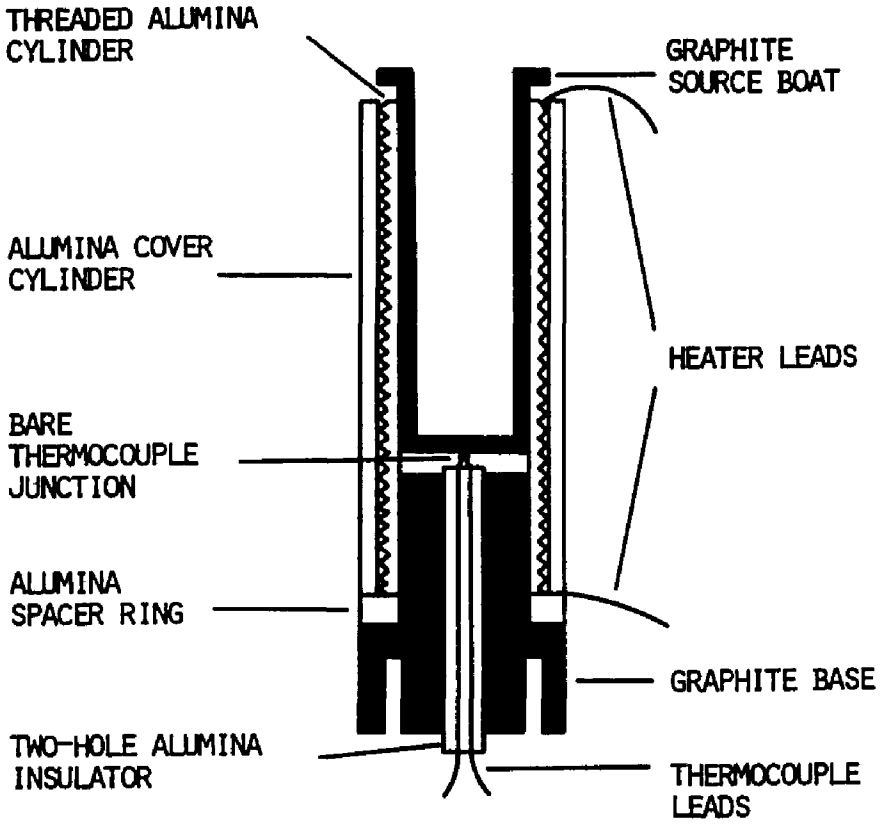

Figure 2.2 Details of the Source Furnace Assembly

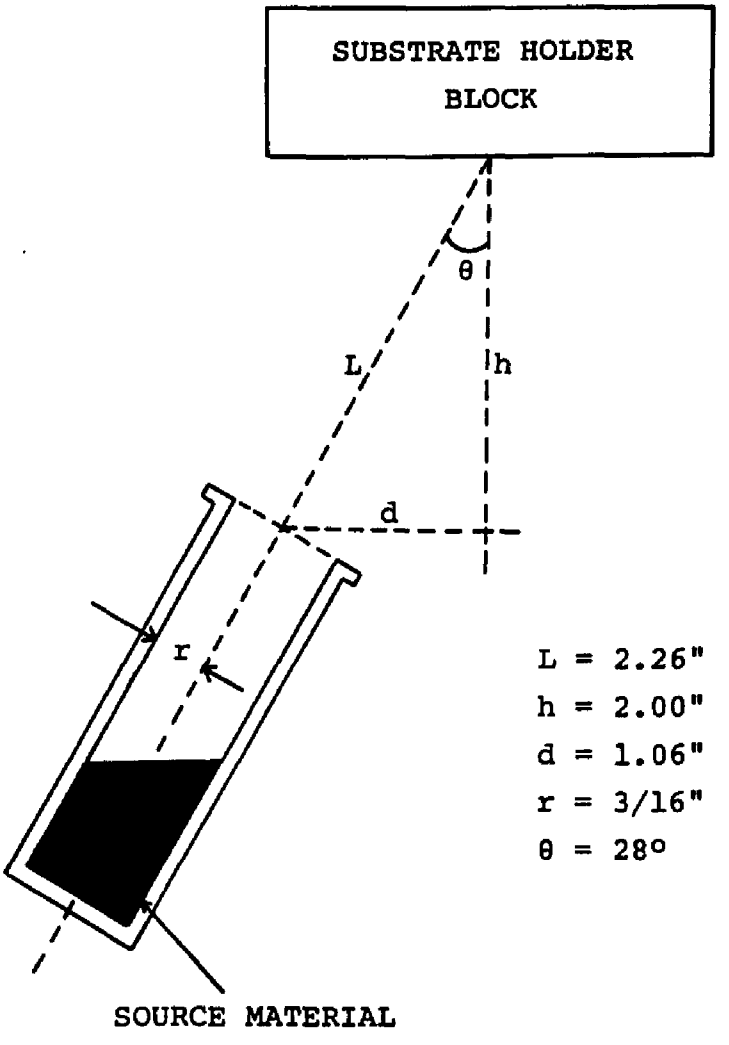

Figure 2.3 Alignment of Source Boat and Substrate Holder Block

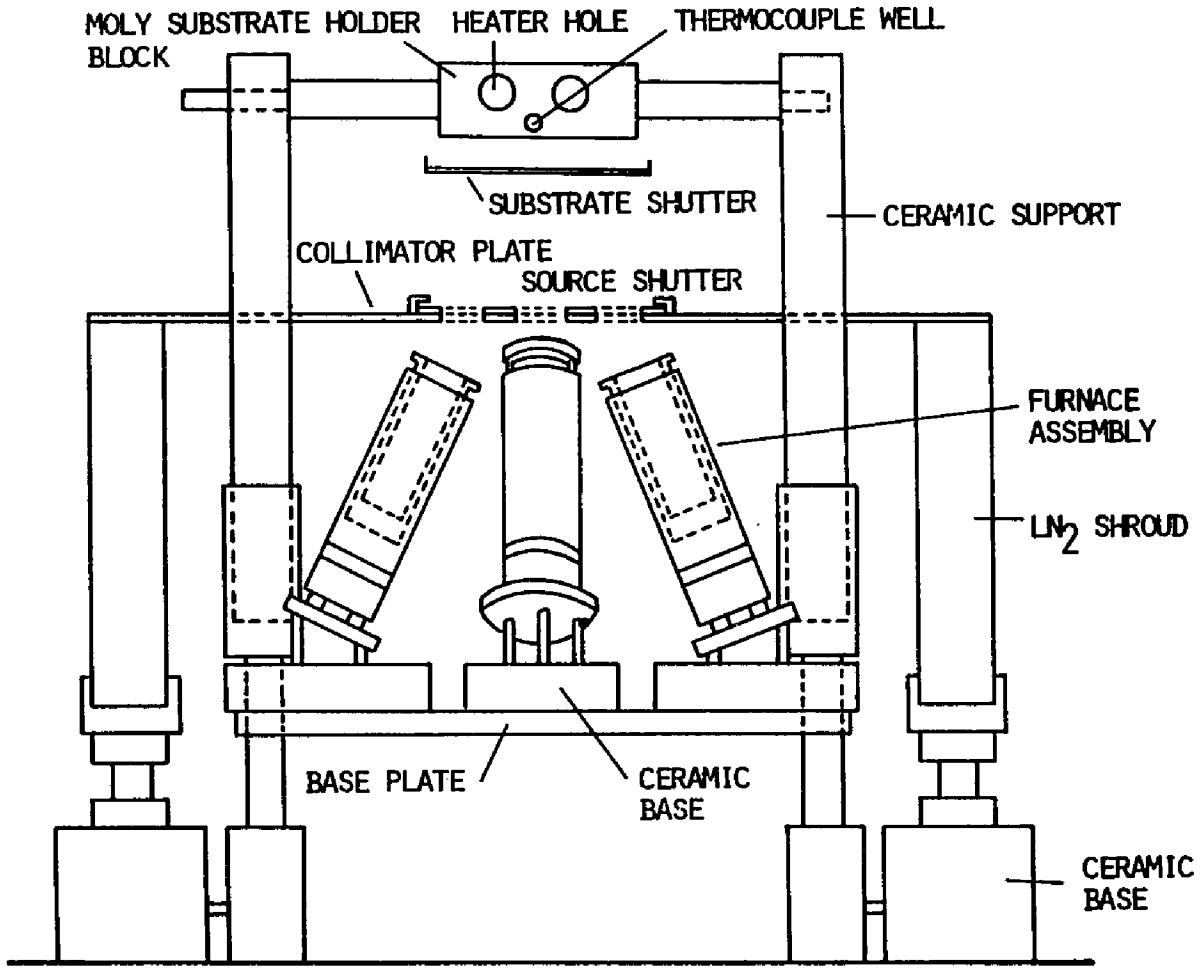

Figure 2.4 General View of the Film Growth Chamber

from others in order to reduce the thermal cross-talk and cross-contamination possibilities. A stainless steel plate with appropriate openings is used as a mechanical shutter for the source furnaces. It is operated from the outside of the growth chamber through a linear motion feedthrough and glides over the collimator plate. The pattern of the holes cut into the shutter plate allows for individual sources or combinations of sources to have their beams turned on or off. Recently one more shutter was added between this source shutter and the substrate holder as a substrate shutter. It will be discussed in more detail in Section 2.5 where the film growth procedures are mentioned. More detailed descriptions of the original system with design criteria is given elsewhere [40].

2.2 Sources and Substrates

Elemental zinc(Zn), tin(Sn), and phosphorus(P) were used as the sources in three seperate source boats. The Zn and Sn were in the form of small shots about 3 mm across in size. They were obtained from Atomergic Chemetals Corp. Initially, Zn shots were used for the Zn source. After a change in the Zn flux control technique, the Zn source material in shot form was replaced by a rod of 10 mm in diameter. This Zn rod source was obtained from Johnson Matthew Inc. The Zn rod was etched in 50 % nitric acid prior to loading into the 9.5 mm diameter source boat. The

phosphorus was in the form of amorphous chucks about 5 mm across in size. It was obtained from Alfa Products. Red phosphorus was used because of its higher stability and low toxicity in comparision to the yellow form. Red phosphorus is known to evaporate primarily as P_4 at temperature up to 600°C [41]. Each source material was certified to be 99.9999 % pure.

Polished fused quartz plates and single crystal (100) GaAs were used as substrates in this research. Commercial grade and optical grade, Optosil I, fused quartz plates 1" x 1" x 1/16" in size obtained from Heraus Amersil were used as substrates. Optosil I quartz substares were used mainly to grow the films of $ZnSnP_2$ for optical measurements. One-side polished GaAs substrates were either semi-insulating Cr-doped GaAs with resistivity value greater than 10^7 Ω-cm or n-type undoped GaAs with resistivity value less than 0.136 Ω-cm. These GaAs substrates were obtained from M/A-COM Laser Diode, Inc. and Material Research Corp., respectively. GaAs substrate with a lattice constant of 5.6533 Å [42] provides an excellent lattice match for the growth of $ZnSnP_2$ whose lattice constant is 5.651 Å [1]. The GaAs substrates were cut into approximately 1 cm^2 in size. Later 1 inch square quartz plates were also cut into about 1.5 cm^2 size pieces to obtain more uniform films on quartz substrates.

2.3 Film Growth Strategy

Research on the MBE growth of III-V binary compound semiconductors have shown that for each element individually impinging on a GaAs substrate, within a reasonable substrate temperature range, the sticking coefficient of Sn flux is near unity, that of Zn flux is lower, and that of P_4 flux is near zero [42-44]. Similar low values of sticking coefficient for Zn and P_4 on quartz crystal have been observed in a study made during the vacuum deposition of Zn_3P_2 [45]. The presence of other elements, however, changes the sticking coefficient of an individual element. For example, the P_4 flux is known to have a higher sticking coefficient in the presence of the Zn flux [45]. Similar comments may also apply to the presence of the Sn flux.

The ratio of Cu/In arrival rates has been found to be critical in order to obtain the stoichiometric films of $CuInSe_2$ and to grow low-resistivity films of $CuInSe_2$ by MBE growth [31]. Our initial runs on $ZnSnP_2$ have shown that the presence of a small amount of Sn significantly changes the sticking coefficient of Zn. From these two observations, the strategy for $ZnSnP_2$ film growth is to critically maintain the desired Zn/Sn arrival flux ratio at the substrate for a given substrate temperature with the requirement on the P_4 flux being somewhat lax so long as an excess of P_4 flux is maintained.

In order for the molecular flow to exist in a source

boat, the condition $\lambda \geq 10d$ must be satisfied where λ is the mean free path of the molecules and d is the diameter of the source boat opening which is 0.95 cm in this case. Table 2.1 shows the estimated mean free path values obtained from the vapor pressure data for each sources materials at various temperatures used in this work [46]. From Table 2.1 it is obvious that the molecular flow conditions will not be completely met for the Zn flux for the Zn furnace temperatures used in this work. It will be even worse for P_4 flux due to its very high vapor pressure for all phosphorus source temperatures used in this work. However. near molecular flow is expected for the Sn flux for the Sn source temperatures used in these experiments.

2.4 Source Flux Considerations

In an effort to grow stoichiometric films of $ZnSnP_2$, a major problem encountered was the reproducibility of the film composition from one run to the next. A number of factors were considered as possible sources of this problem. These included substrate surface contamination, residual background pressure, contamination of sources due to the flux cross-talk, and the variation in the arrival of elemental fluxes.

Cho and Arthur reported that the carbon and oxygen revealed from Auger Electron Spectroscopy (AES) were the main contaminants on the surfaces of GaAs and quartz

Table 2.1 Estimated Mean Free Path λ for each Source Material at various Furnace Temperatures.

Molecule	Source Furnace Temperature (°C)	Mean Free Path(cm)
Zn	260	27.97
	280	10.10
	300	3.92
	320	1.63
Sn	1000	121.86
	1020	79.76
	1040	52.89
	1060	35.52
P_4	290	9.79×10^{-4}
	310	4.09×10^{-4}
	330	1.86×10^{-4}
	350	8.77×10^{-5}

substrates[42]. As suggested by them [42], the cleaned GaAs substrate surfaces were etched in 1:1:10 volumes of H_2SO_4: H_2O_2: H_2O for 20 seconds, rinsed in deionized water, and dried with an inert gas jet just before they were loaded into the growth system to reduce the carbon content from the surfaces. The GaAs substrates were also heated to 450-500°C for 3 to 5 minutes prior to film growth in order to reduce the oxygen from the substrate surfaces. The cooling method for the shroud which surrounds the furnace assemblies had been changed from chilled water to liquid nitrogen in order to reduce the background pressure. This change reduced the background growth pressure from about $3x10^{-6}$ Torr to about $4x10^{-7}$ Torr. The three source furnaces were completely isolated from the sides by welding three stainless steel partitions onto the underside of the collimator plate in order to eliminate the flux cross-talk underneath the collimator plate. However, these changes did not make significant improvements on the reproducibility of the film composition.

Sn fluxes and Zn fluxes with and without substrate holder block in position were measured to check the stabilities of those fluxes with time. A decline in the Zn flux with time for this system had been observed and the possible causes have been suggested [40]. Those measurements had been performed without substrate holder block in position using UTI Model 100C quadrupole mass

analyzer. The use of Ti-Ball sublimation pump as suggested in [40] did not improve the Zn flux decrease with time. In addition to a UTI 100C precision mass analyzer an AMETEK/Dycor Electronic's Model M200M quadrupole mass analyzer was attached to the top of the growth chamber to measure Zn flux and utilize its analog output signal for plotting on the strip chart recorder. The independent measurements on Zn flux using M200M quadrupole analyzer showed significant flux variations from one run to the next as well as the decrease in flux with time for each run. Figure 2.5 shows the typical Zn flux decay with time. In this figure, the Zn source shutter was opened at time t=0. In order to reduce the amount of Zn flux decrease with time the Zn source boat was covered with a graphite lid as shown in Figure 2.6. The purpose of this modification was to possibly reach the equillibrium vapor pressure condition inside the source boat as reported by others [47]. In this work, the lid did not seem to eliminate this problem at all. Instead, it showed severe flux oscillations. The small volume of source boat in this work of about 2.7 cm^3 compared to the volume of the boat of about 25 cm^3 reported in the other work [47] may be the reason that this special shape lid did not work in our case. Also, contamination of the evaporating surface is known to affect the rate of evaporation [48]. Hence, the fresh Zn source drops were etched in nitric acid, rinsed in deionized water, and blown

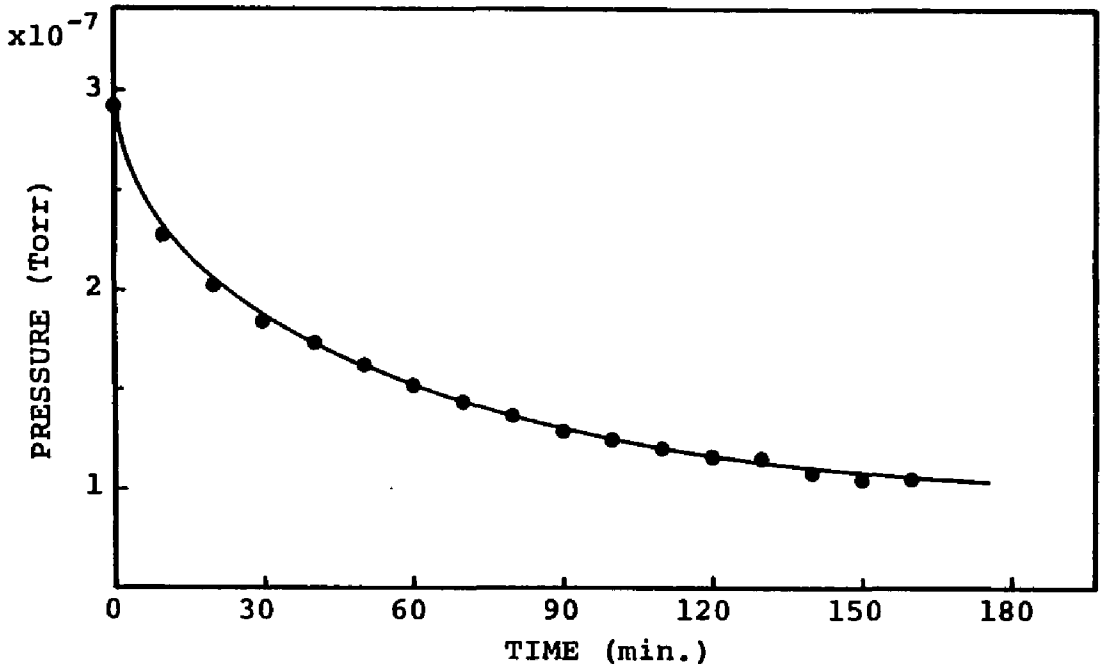

Figure 2.5 Zn Flux Variation with Time at the Quadrupole Probe for the Zn Furnace Temperature of 300^{o}C

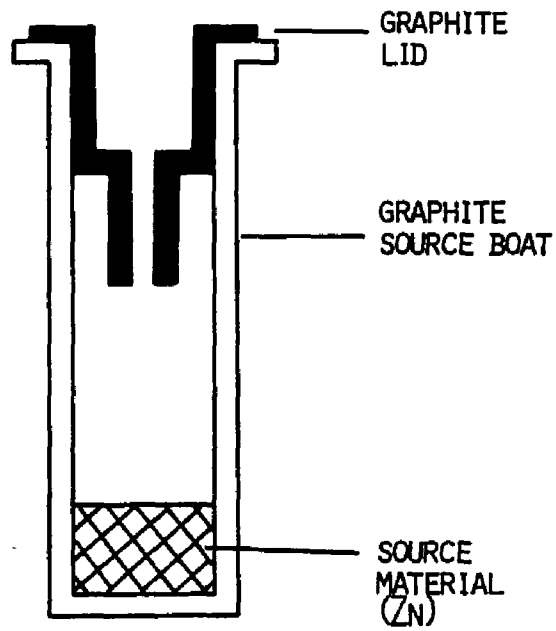

Figure 2.6 Zn Source Boat with Graphite Lid

dry with prepurified nitrogen gas just before they were loaded into the system as described in [49] to reduce possible surface contamination. It, however, did not alleviate the problem of Zn flux decay with time. The decision, therefore, was made to control the Zn flux directly instead of controlling the Zn source furnace temperature. Eurotherm Model 820 microprocessor based temperature controller with an option of 0-10 VDC input capability was obtained to use the analog output signal from an AMETEK/Dycor M200M quadrupole mass analyzer as an input to the controller. Figure 2.7 is a schematic diagram of the Zn flux control system. With this control scheme, Zn flux of less than ±2.5% deviation with time has been achieved. Figure 2.8 shows a plot of the measured Zn partial pressure and the Zn source furnace temperature with time. The quadrupole gain was calibrated for each measurement throughout the entire experiment.

2.5 Film Growth Procedure

The substrates were dipped in cold trichloroethylene for 10 minutes to remove the excess organic contaminants and degreased in hot trichloroethylene and hot acetone for 5 minutes each, rinsed in deionized water and methanol. They were subsequently dipped in dilute 10% HF solution for 1 minute for GaAs substrates and for 10- 15 seconds for quartz substrates, rinsed in deionized water, flush dried with

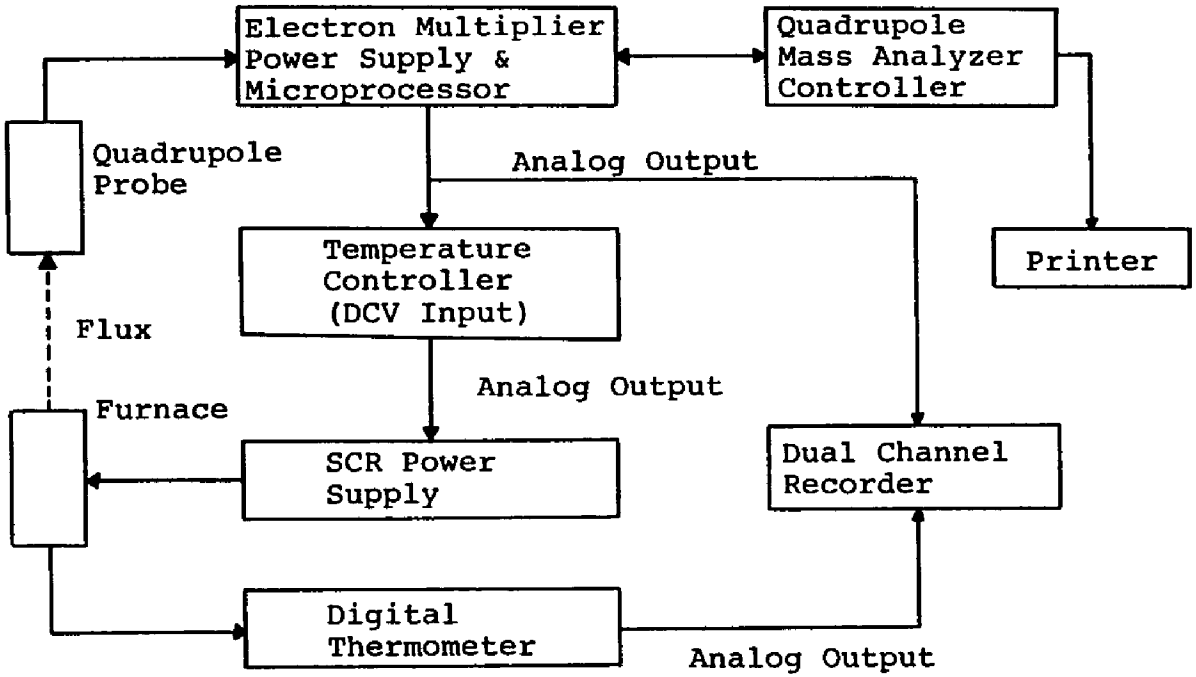

Figure 2.7 Schematic Diagram of the Zn Flux Control Setup with a Quadrupole Mass Analyzer

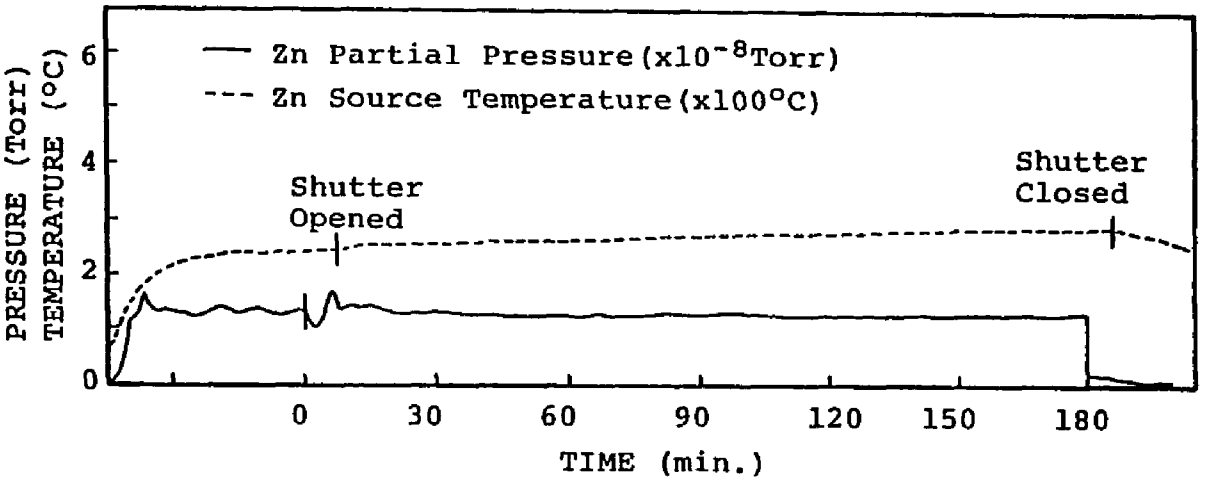

Figure 2.8 Zn Source Furnace Temperature and Zn Partial Pressure with Time

prepurified nitrogen gas, and stored in methanol till use. GaAs Substrates were again etched in an etching solution of H_2SO_4: H_2O_2: H_2O = 1: 1: 10 by volume for 20 seconds to reduce the carbon content from the surfaces just before they were installed into the growth system. Whenever the Zn source was exposed to the ambient air, the Zn source was also etched in a dilute 10% HF solution for 1 minute followed by rinse in deionized water and flush dried with prepurified nitrogen gas to eliminate the possible oxide layer.

After the three sources were loaded and a cleaned substrate was installed, the system was pumped down to a background pressure of about $7x10^{-7}$ Torr which takes about 24 hours. The system was outgassed by circulating hot water through the growth chamber walls. Then the chamber walls were cooled down by circulating cold water. Subsequently, the cryotrap was filled with liquid nitrogen and the Ti-Ball sublimation pump was turned on. Thirty minutes after turning the sublimation pump on, the LN_2 shroud was filled . After these procedures the background pressure of the growth chamber reduced to about $9x10^{-8}$ Torr or lower.

The temperatures for the substrate and the source furnaces were increased incrementally to their desired final values so as to avoid flux overshoots resulting from the controller overshoots. First, the substrate heater was turned on. When the substrate temperature reached 240°C,

the Sn furnace was turned on. When the Sn furnace reached 800°C, power to the Zn source was turned on and the Zn furnace was allowed to reach 180°C. At this point, phosphorus furnace was turned on and allowed to reach its final temperature value. During these power-on procedures, the mechanical source shutter on the collimator plate was partially opened when the Zn boat temperature reached 220°C. This opened the Sn and the Zn sources only while the phosphorus source remained closed. From this point onward the M200M quadrupole probe took over the control of the temperature on the Zn source. The probe measures Zn partial pressure and sends the analog output to the temperature controller to maintain the constant Zn flux. At least 30 minutes were allowed after all the heaters reached their desired temperatures to stabilize the source fluxes prior to starting the film growth. Then the shutters for the sources and the substrate were opened simultaneousely to start the film growth. The shutters were kept open for the desired length of time.

At the end of the growth run, the shutters were completely closed and all the heaters were shut off. The Ti-Ball sublimation pump was kept on for at least 30 minutes to keep the system pressure low while the source boats cooled down. The system was allowed to cool overnight in order to reduce the phosphorus pressure prior to its exposure to air for substrate removal and reloading

purposes.

2.6 Electrical Contacts

Different metals were tried in order to form electrical contacts to the grown films of $ZnSnP_2$. Sn was used to make an ohmic contact to GaAs substrate. Sn itself has very little adhesion to the clean GaAs substrate. To increase the adhesion strength of Sn onto GaAs substrate, $SnCl_2$ solution was used as described by Schwartz and Sarace [50]. $SnCl_2$ disolved into acetone was used as a flux. The I-V response between two Sn contacts made on n-type GaAs substrate is shown in Figure 2.9.

Indium was used to make contacts to $ZnSnP_2$ films. Approximately 1000 Å of Indium was first deposited by vacuum evaporation on the grown layer of $ZnSnP_2$. It was then heated at 170°C for 15 sec. in an argon atmosphere with a small In-ball on top of the vacuum deposited In. This contact showed slightly non-linear response. However, the contact resistance was quite high. Evaporated silver was also tried to make contact to the grown $ZnSnP_2$ layer. Ag contacts without heat treatment appeared to have less resistance than the heat-treated In contacts. Figures 2.10 and 2.11 are the I-V responses between two heat-treated In contacts and between two vacuum deposited Ag contacts, respectively. These curves appear somewhat similar to the curves obtained on contacts formed by a tunneling junction

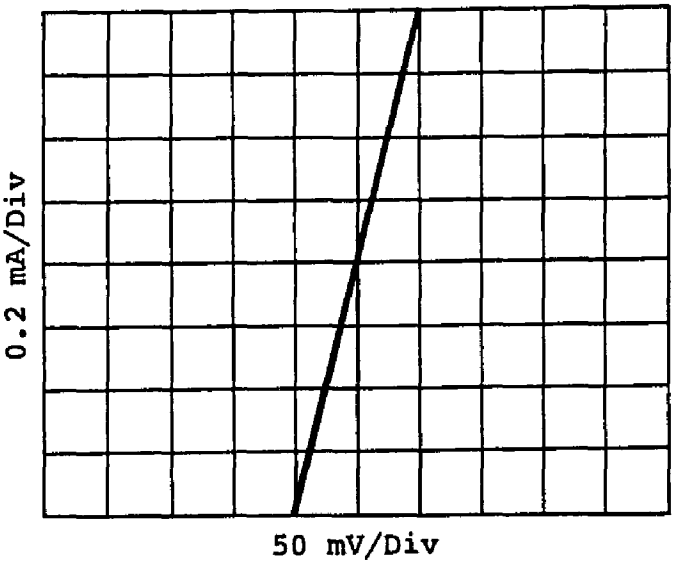

Figure 2.9 I-V Characteristics Between Two Sn Contacts on n-type GaAs Substrate

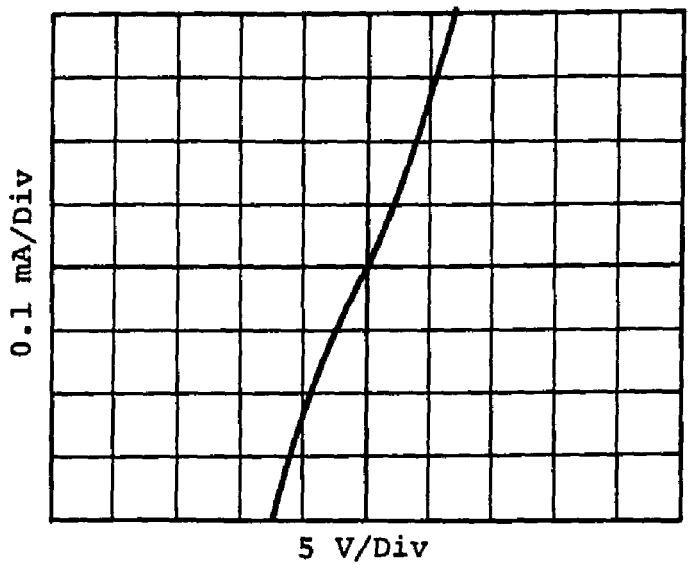

Figure 2.10 I-V Characteristics Between Two Heat-Treated In Contacts on $ZnSnP_2$ Film

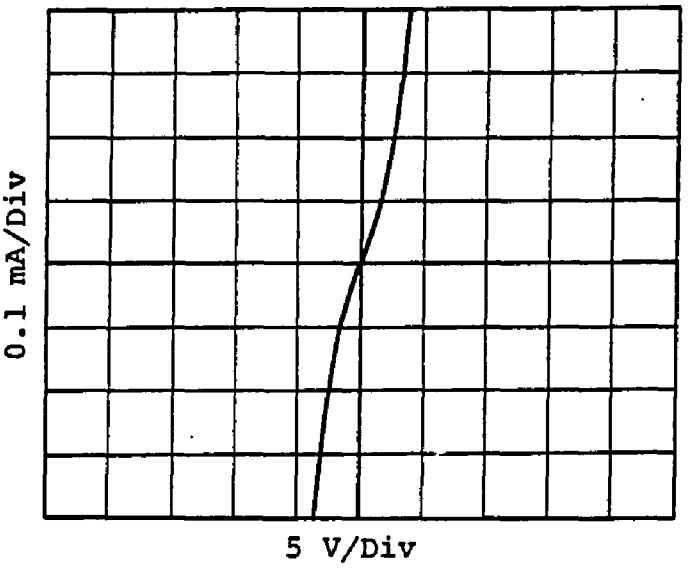

Figure 2.11 I-V Characteristics Between Two Vacuum Deposited Ag Contacts on $ZnSnP_2$ Film

[51]. Platinum has been used by others to make an ohmic contact by welding Pt wire to the bulk sample of $ZnSnP_2$ grown by traditional solution growth method [52]. However, no attempt has been made to make an ohmic contact using Pt to films grown in this work. Recently, Au with 1% Be has been reported to make good quality contact to $ZnSnP_2$ film [23]. In this work, Ag was used as the material for electrical contacts for resistivity and Hall measurements for most of the samples.

CHAPTER 3

RESULTS AND DISCUSSIONS

3.1 Film Growth Conditions

The first successful film was grown with Zn, Sn, and P source temperatures at 308°C, 950°C, and 310°C respectively. The substrate temperature was 265°C. The later is much higher than the reported substrate temperature values of <80°C for nucleation and <185°C for subsequent growth of vacuum evaporated Zn_3P_2 films [45]. In this work, growth at substrate temperature of 260-290°C has been obtained on GaAs substrates while growth has been obtained up to a temperature of 310°C on quartz substrates.

The optimum growth parameters for near stoichiometric film growth were respectively 320°C, 1025°C, and 310°C for the Zn, Sn, and phosphorous source boat temperatures. The substrate temperature was at 275°C. However, the reproducibility of film composition was a serious problem with the growth process. After the change of the Zn flux control method, the optimum growth parameters for near stoichiometric film growth became 1.1×10^{-8} Torr for partial pressure of Zn flux as measured by the quadrupole mass analyzer, and 1025°C, 340°C, and 280°C for Sn source, P source, and for substrate temperatures respectively.

The Zn flux at the quadrupole probe has been estimated to obtain the ratio of Zn flux to Sn flux at the substrate

based on the kinetic theory which provides a relationship between partial pressure and impinging flux [48]. After calculation of the Zn flux at the quadrupole probe, appropriate geometrical factor was applied to estimate the Zn flux at the substrate surface. Sn flux at the substrate at the optimum temperature has also been calculated using the cosine law by assuming Knudsen cell [48]. The equillibrium vapor pressure needed in this calculation has been obtained from the following equation [41]

$$\log p = A - B/T + CT + D\log T \qquad (3.1)$$

for a given temperature T where A, B, C, and D are constants and given in Table 3.1, p is in Torr, and T is in °K. From these calculations the estimated critical ratio of Zn/Sn fluxes at the substrate for near stoichiometric film growth revealed to be in the range of 3.5-4.7 due to the scattered molecules from the chamber walls.

In order to determine the film growth rate, the weight gain of the substrate was carefully monitored by weighing the substrate before and after the growth run. The growth rate for each run has been determined from this weight gain analysis. The average film growth rates on GaAS substrates were in the range of 50-70 Å/min. while the average growth rates on quartz substrates were in the range of 60-90 Å/min. In the calculation of film growth rate, the grown film was assumed to be uniform and to have stoichiometric composition. The lower film growth rate on GaAs substrates

Table 3.1 Coefficients of Equation (3.1) for Elements Used in This Work.

Element	Coefficients			
	A	B	C	D
Zn	13.50846	7011.863	0.00040185	-1.58311
Sn	-9.32188	14023.92	-0.00088122	5.62012
P	36.01066	8053.440	0.00116106	-7.86743

may be due to a possible preferred directional growth because of good lattice match between $ZnSnP_2$ films and GaAs substrates.

3.2 Surface Morphology

The film growth system used in this work was designed to grow uniform films on substrates of about 1 cm^2 in area [40]. Hence, the films grown on 1 inch square quartz substrates were visibly inhomogeneous. Small quartz substrates of about 1.5 cm^2 area were used in the later stages of this experiment to obtain more homogeneous films and to conserve the substrate material.

The grown films were examined under optical microscope just after unloading from the growth system. Four colors, in general, were observed on the surfaces of the grown films in these experiments. These are dark brown, whitish gray, dark gray, and near black. The surfaces of the grown films along with their textures could be classified into three groups. They are powdery, silvery metal-like, and smooth and reflecting layers. The dark brownish films were always powdery and the whitish gray films were silvery metal-like. The near black films were either powdery or were smooth and reflecting. However, the dark gray films were mostly smooth and reflecting layers. The dark brownish and powdery layers were frequently found from the films grown on the quartz substrates in the early stages of the work. The brownish

and powdery layers were seldom observed on the films grown on the GaAs substrates. The whitish gray films were also mainly observed on the films grown on the quartz substrates.

Scanning Electron Microscope (SEM) pictures were taken from the surfaces of the grown films to relate the microscopic surface morphology to the film compositions obtained from Energy Dispersive Spectroscopy (EDS) analysis carried out at the same locations on the films. The dark brownish and powdery films obtained mostly on quartz substrates and rarely on GaAs substrates were found to be Zn-rich from the EDS analysis. Their surfaces under SEM exhibited dendritic needle-like growth as shown in Figure 3.1 and Figure 3.2. Figure 3.1 shows the surface of a Zn-rich and Sn deficient film while Figure 3.2 shows the surface of a Zn-rich and P-deficient film. Studies on the SEM pictures also showed the characteristic structures of the Zn-deficient films. Decreasing the Zn content from the stoichiometric amount made the film surfaces look near black and more powdery. Under SEM these surfaces showed no needle-like structures as seen in Figures 3.3 and 3.4. Figures 3.3 and 3.4 show the surface structures of the Zn-deficient films with Sn-rich and with P-rich components, respectively. The near stoichiometric films were dark gray in color having a smooth and reflecting surface structure. These films showed continuous but slightly rough surfaces under SEM as depicted in Figures 3.5 and 3.6. Figure 3.5

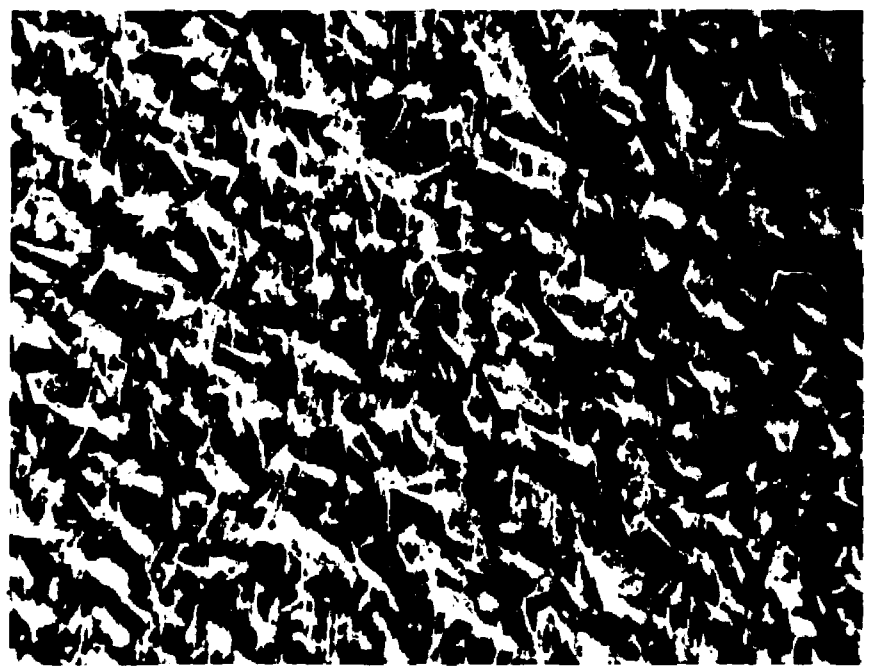

Figure 3.1 SEM Picture of a Zn-rich and Sn-deficient Film on a Quartz Substrate (x2500 Magnification)

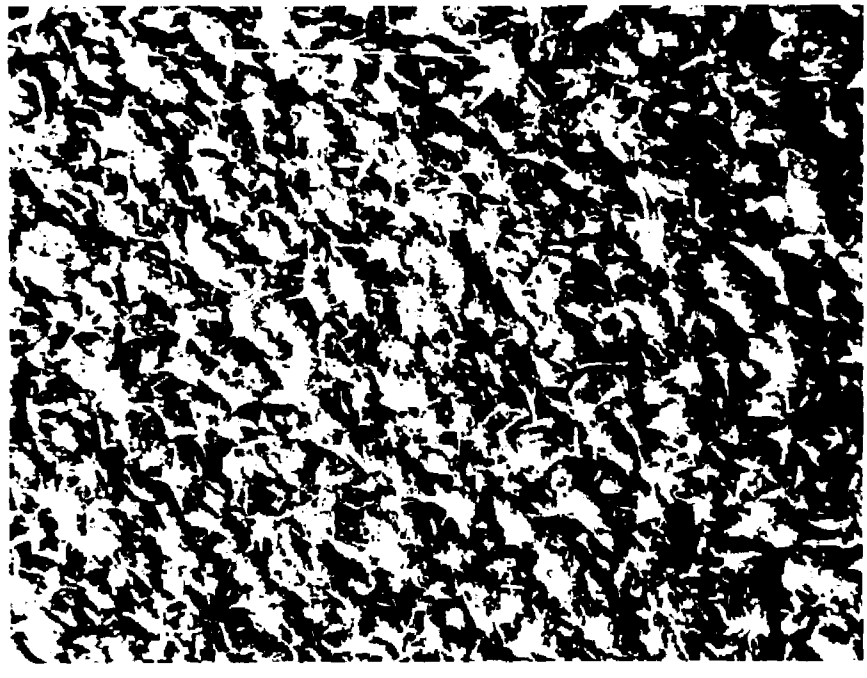

Figure 3.2 SEM Picture of a Zn-rich and P-deficient Film on a GaAs Substrate (x3500 Magnification)

Figure 3.3 SEM Picture of a Zn-deficient and Sn-rich Film on a GaAs Substrate (x2500 Magnification)

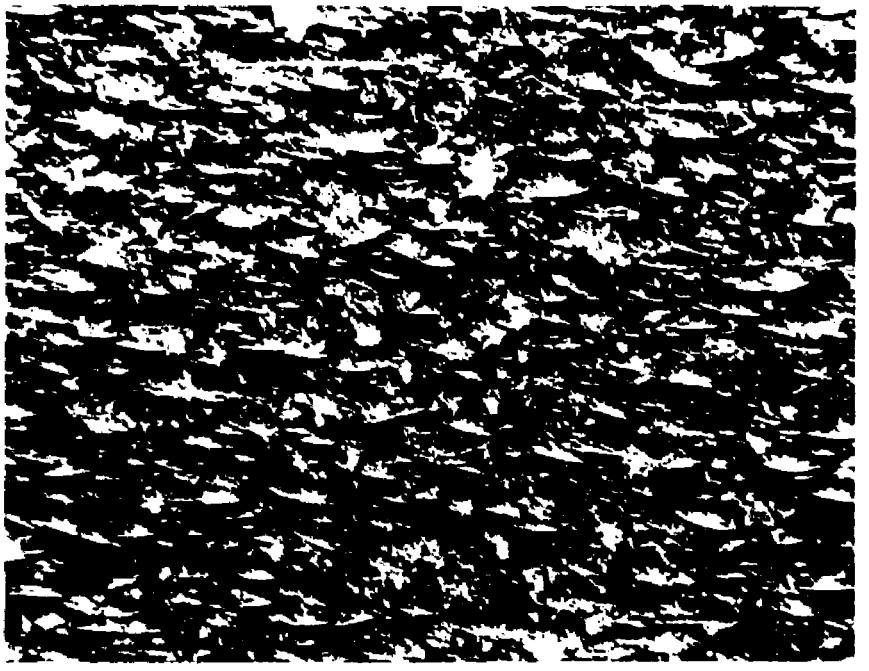

Figure 3.4 SEM Picture of a Zn-deficient and P-rich Film on a GaAs Substrate (x2500 Magnification)

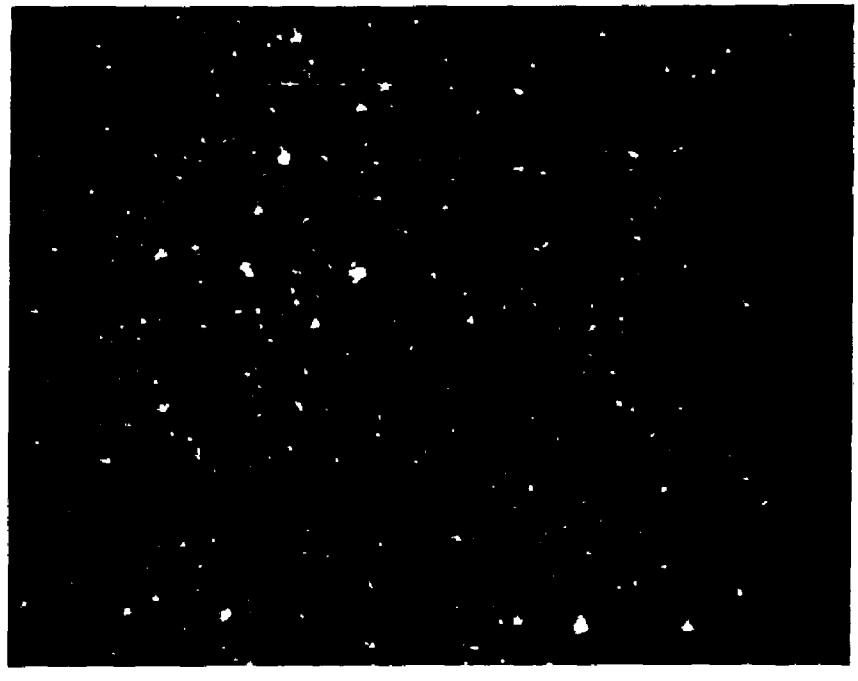

Figure 3.5 SEM Picture of a Near Stoichiometric Film on a GaAs Substrate (x2500 Magnification)

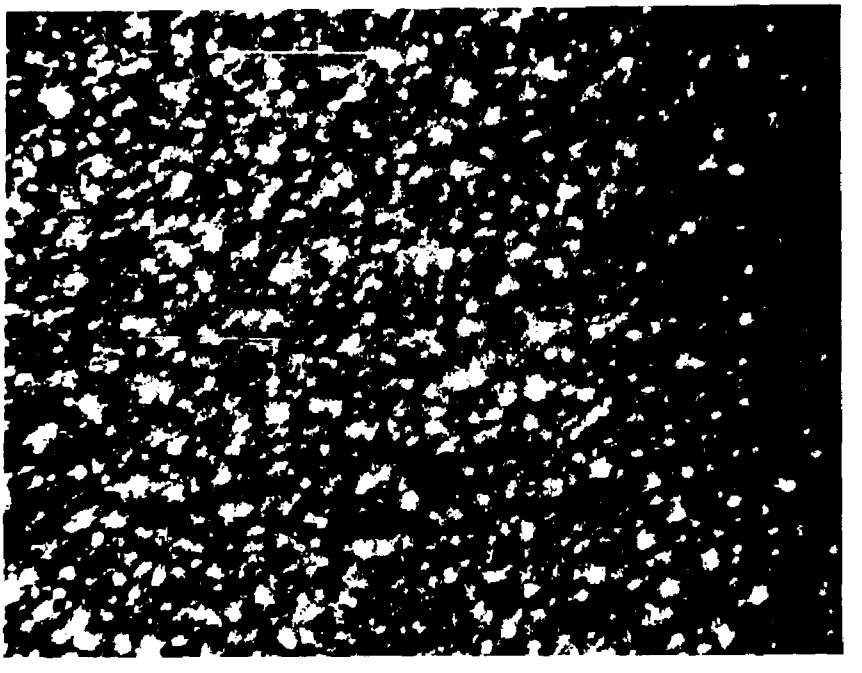

Figure 3.6 SEM Picture of a Near Stoichiometric Film on a Quartz Substrate (x2500 Magnification)

is the surface of a near stoichiometric film grown on a GaAs substrate and Figure 3.6 is the surface of a near stoichiometric film grown on a quartz substrate. From this studies, it was observed that the film surface morphology was most sensitive to the Zn content in the grown films. The atomic compositions of the films shown in Figures 3.1 to 3.6 are presented in Table 3.2.

3.3 Composition Analysis

A number of films were analyzed using EDS on the Phillips Electronics Instruments Model EDAX 9100 to determine the atomic compositions of the grown films. The EDS analyzed atomic compositions in percent were used in adjusting the growth parameters for the next growth run. A partial listing of the atomic compositions of the grown films as determined by EDS is given in Table 3.3. All the values in Table 3.3 are the average values over the film surfaces. As shown in Table 3.3, films within a few percent of the desired stiochiometry were routinely obtained. However, the variation in the exact atomic composition from one run to the run was a problem encountered throughout the entire film growth experiments. Similar problems with vacuum growth of ternary compound semiconductors have been experienced by others while growing thin films of $CuInSe_2$ [30,31].

Some of the films were analyzed by the method of Wave

Table 3.2 Atomic Compositions of the Films Shown in Figures 3.1 - 3.6 as Obtained from EDS Analysis.

Figure No.	Atomic Composition (%) Zn	Sn	P
3.1	49.85	7.12	43.03
3.2	45.91	25.45	28.64
3.3	22.97	29.64	47.38
3.4	10.03	26.00	63.97
3.5	26.12	25.25	48.63
3.6	25.11	26.93	47.96

Table 3.3 Average Atomic Composition of Some films from EDS Analysis.

Sample No.	Atomic Composition (%) Zn	Sn	P
35ZSP/GA	24.08	26.31	49.61
45ZSP/GA	25.26	29.20	45.54
52ZSP/CQ	24.20	28.23	47.57
57ZSP/GA	24.92	27.35	47.73
58ZSP/GA	22.07	27.11	50.82
60ZSP/GA	27.75	28.67	43.58
62ZSP/GA	24.57	28.77	46.66
64ZSP/CQ	23.71	28.05	48.24
66ZSP/GA	22.83	29.00	48.17
78ZSP/GA	26.12	25.25	48.63
89ZSP/CQ	25.11	26.93	47.96
95ZSP/OQ	24.20	27.23	48.57
104ZSP/GA	23.79	28.13	48.08
105ZSP/GA	23.76	28.44	47.80

Dispersive Spectroscopy (WDS) at the Solar Energy Research Institute (SERI). The EDS analysis results on some films deviated by more than 10% from the WDS analysis results. For example, the average atomic compositions of the sample No. 83ZSP/GA from EDS analysis were 27.36% of Zn, 37.67% of Sn, and 34.97% of P as compared to 22.21% of Zn , 29.42% of Sn, and 48.37% of P for the same film from the WDS analysis. The reason for this is not yet known. However, in most cases, the WDS analysis results agreed well with the EDS analysis results within a few percent deviations. WDS, in general, is known to be a better tool for the quantitative analysis when compared to EDS.

Some of the near stoichiometric films were very uniform in composition over the entire surface of the film. Tables 3.4 and 3.5 give the WDS analysis results for the near stoichiometric films grown on a GaAs substrate and on a quartz substrate respectively. The percentage variation in composition is less than ±5% for the films whose data are given in Table 3.4 and 3.5. On some of the more uniform films grown on GaAs substrates, less than ±0.75% variation in the atomic composition has been obtained for each of the three elements across a 1 cm^2 on the grown film. As seen from the WDS and the EDS results, the grown films contained a little less than the stoichiometric amount of P in most cases.

Auger Electron Spectroscopy (AES) analysis was

Table 3.4 Atomic Composition from WDS Analysis on Sample No. 78ZSP/GA for 10 Equally Spaced Points along the Diagonal of the Sample.

Position No.	Atomic Composition (%) Zn	Sn	P
1	26.69	24.83	48.48
2	27.21	26.62	46.16
3	26.05	25.14	48.81
4	26.25	25.25	48.51
5	26.24	25.31	48.45
6	26.15	25.47	48.38
7	25.99	25.24	48.77
8	25.85	25.33	48.82
9	25.27	25.47	49.26
10	26.69	25.13	48.18
Average	26.24	25.38	48.38

Table 3.5 Atomic Composition from WDS Analysis on Sample No. 89ZSP/CQ for 10 Equally Spaced Points along the Diagonal of the Sample.

Position No.	Atomic Composition (%) Zn	Sn	P
1	27.02	25.80	47.18
2	26.18	26.41	47.40
3	25.33	26.73	47.93
4	25.50	27.38	47.12
5	25.11	27.13	47.76
6	24.87	27.49	47.65
7	24.86	27.51	47.64
8	24.85	27.80	47.35
9	25.17	27.56	47.27
10	25.62	27.56	46.82
Average	25.45	27.14	47.41

performed on some of the films at SERI to identify the possible surface and bulk contaminants and to see the compositional depth profiles of the grown films. AES analysis revealed carbon and oxygen as the major surface and bulk contaminants. At the surface of the films the concentrations of the carbon and the oxygen were higher than those in the bulk of the films. The actual sources of the carbon and the oxygen are not obvious but the carbon could come from the oil vapors of the mechanical pump and the diffusion pump, and the oxygen probably could come from the residual background ambient. In most samples analyzed by AES, the concentrations of P and Zn just underneath the film surface were lower than those on the bulk of the films. The decrease in the surface concentration of Cu had been reported in MBE grown $CuInSe_2$ [30]. The increase of Sn concentration just underneath the film surface is similar to the reported result of the segregation of Sn on the surface of the epitaxially grown GaAs [53].

Figures from 3.7 to 3.9 show the typical composition depth profile plots obtained from the AES analysis. Figure 3.7 is the AES depth profile from the films grown with Zn source temperature control. It shows the decrease of Zn content near the film surface indicating a decrease in the Zn flux with time. Figures 3.8 and 3.9 show the AES depth profiles of the sample No. 67ZSP/GA and 83ZSP/GA on GaAs substrates respectively which were grown with Zn flux

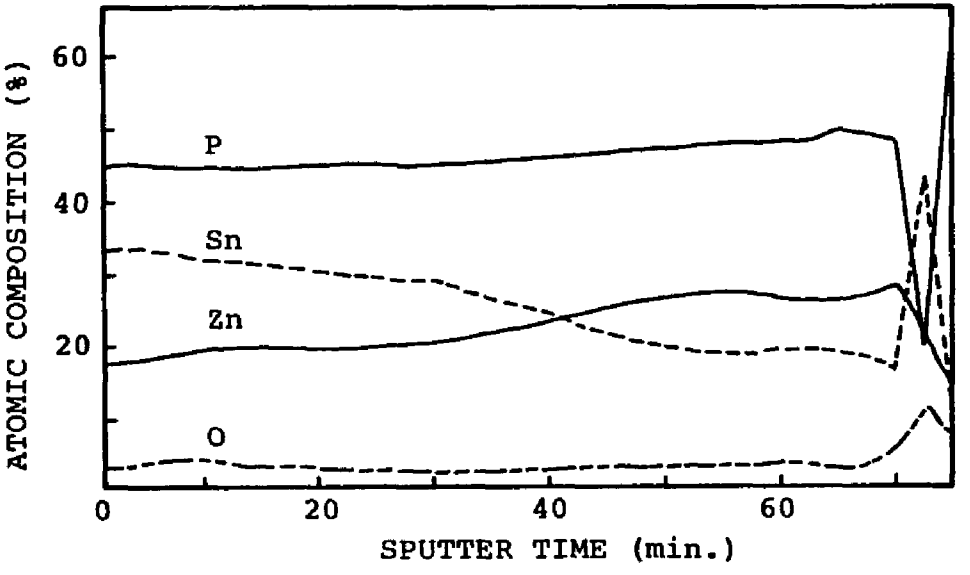

Figure 3.7 Typical AES Depth Profile for Films Grown with Zn Source Temperature Control (Sample No. 5ZSP/CQ)

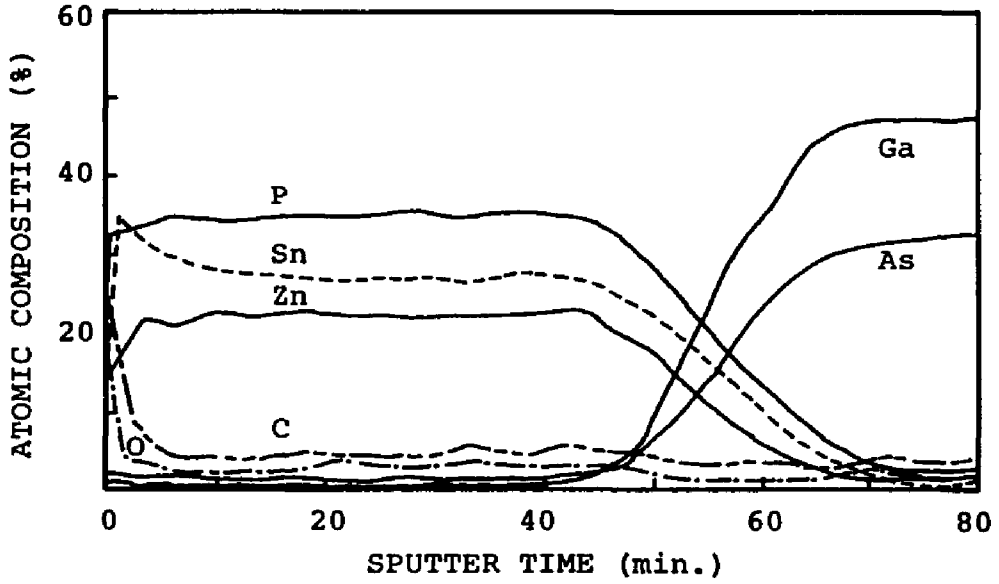

Figure 3.8 AES Depth Profile for a Film Grown on a GaAs Substrate with Zn Flux Controlled by the Quadrupole Probe (Sample No. 67ZSP/GA)

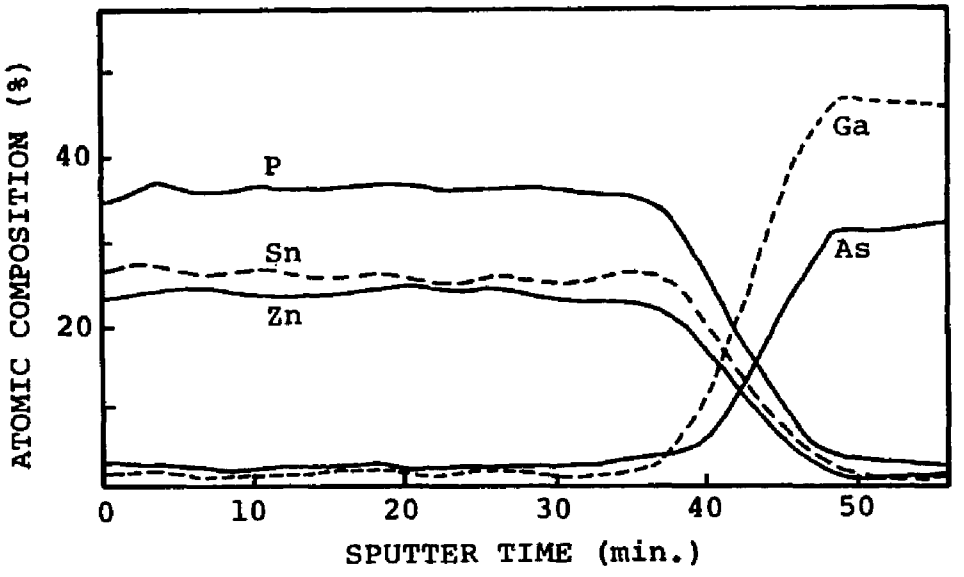

Figure 3.9 AES Depth Profile for a Film Grown on a GaAs Substrate with Zn Flux Controlled by the Quadrupole Probe (Sample No. 83ZSP/GA)

control. The higher surface concentrations of the carbon is evident especially in Figure 3.8. AES analysis results showed that the grown films have reasonable degree of compositional uniformity along the depth of the films.

3.4 Optical Analysis

$ZnSnP_2$ films grown on optical grade clear quartz substrates, Optosil I, were examined qualitatively and quantitatively by the transmission spectroscopy to see the existence of an optical absorption edge and to estimate the value of the energy gap of the grown films. Applied Physics Corporation's Cary Model 14 Spectrophotometer was used to measure the optical absorption spectra in the wavelength range from 350 nm to 1500 nm. Single crystal $ZnSnP_2$ is known to have a direct band gap of 1.66 eV corresponding to a wavelength of 748 nm in the near infrared.

Initial experiments showed that the films with growth time of more than 2 hours were too thick to allow any measurable transmission. The possible reasons for this high value of absorption may be the scattering effects due to the film surface roughness in addition to the absorption itself. The optical absorption coefficient, α, versus incident photon energy was determined for several very thin films grown on Optosil I quartz substrates. Absorption coefficient of greater than 10^5 cm^{-1} were observed on these films without considering the scattering effects at the film

surfaces. Figure 3.10 shows the typical results of this analysis. The extra absorption below the band gap is probably due to defects in the film. For an allowed direct bandgap transition, the absorption coefficient can be related to the photon energy [54] by

$$\alpha h\nu = A(h\nu - E_g)^{1/2} \qquad (3.2)$$

where A is a constant and E_g is the energy gap. Therefore, for a direct bandgap semiconductor, the $(\alpha h\nu)^2$ vs. $h\nu$ characteristics is predicted to be a straight line, with a photon energy axis intercept indicative of the bandgap. The straight line extrapolation of the (Absorption Coefficient x Photon Energy)^2 versus incident photon energy indicates that the grown film has a direct bandgap of 1.62 eV. From the Figure 3.10 and the equation (3.2) the proportional constant A was determined to be 1.5×10^6 $(eV\text{-}cm^2)^{1/2}$. The growth parameters for the film in Figure 3.10 were 1×10^{-8} Torr for Zn partial pressure, 1025°C and 340°C for Sn and P source furnace temperatures, and 285°C for substrate temperature. The growth time was 1.5 hours. The film composition from EDS analysis was 24.20% of Zn, 27.23% of Sn, and 48.57% of P. The observed value of 1.62 eV is close to the generally accepted value of 1.66 eV for the single crystal material. The small discrepancy may be due to the slight stoichiometric variations in the film composition, disorder and large number of defects in the film, or to a possible presence of a phase mixture.

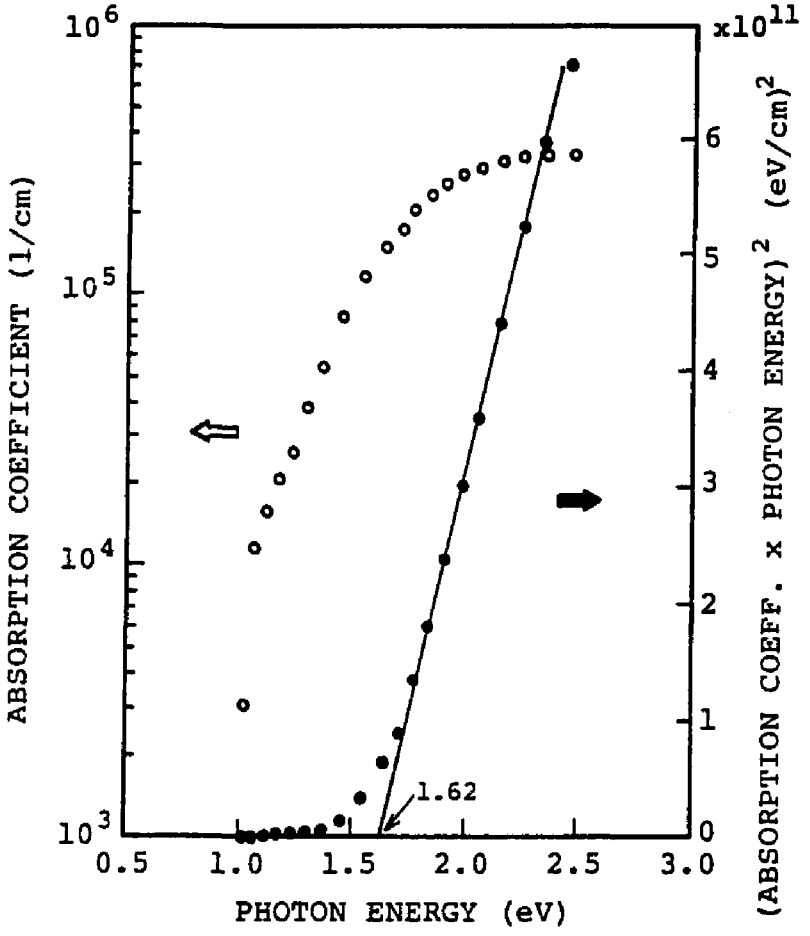

Figure 3.10 Optical Absorption Coefficient vs. Photon Energy for Sample No. 95ZSP/OQ

3.5 X-Ray Diffraction Analysis

X-Ray diffraction measurements were made on the films grown on (100) GaAs substrates and on fused quartz substrates with 1.5418 Å Cu K_α radiation. Phillips Instruments Model APD 3500 with a single crystal diffractometer was used for these measurements. Figures 3.11 and 3.12 show the typical diffraction spectra from the films grown on the quartz substrates and the films grown on the (100) GaAs substrates respectively. The theoretical relative intensities of the X-Ray powder diffraction peaks for the chalcopyrite $ZnSnP_2$ and for the Zinc Blende $ZnSnP_2$ were calculated to identify the structure of the grown films because no standard X-Ray diffraction spectrum of chalcopyrite $ZnSnP_2$ is available at the present time. The results of calculations and the comparisions are presented in Table 3.6. The details of the calculations are given in the APPENDIX. The diffraction spectra obtained from measurements agree well with the spectrum of the theoretically calculated relative intensities of the X-Ray powder diffraction peaks for chalcopyrite $ZnSnP_2$ except for the (400) diffraction peak from the film grown on (100) GaAs substrate. This peak is attributed to the superposition of the diffracted X-Ray beam from the grown film and from the GaAs substrate as the X-Ray diffraction from the single crystal (100) GaAs substrate showed the highest peak at

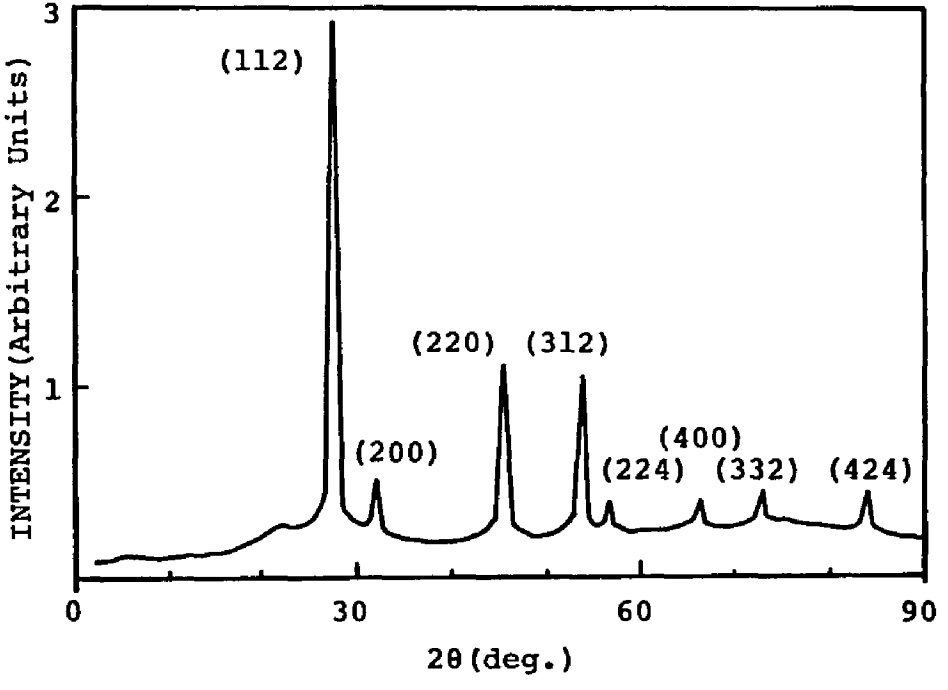

Figure 3.11 X-Ray Diffraction Spectrum of $ZnSnP_2$ Film Grown on Quartz Substrate (Sample No. 90ZSP/CQ)

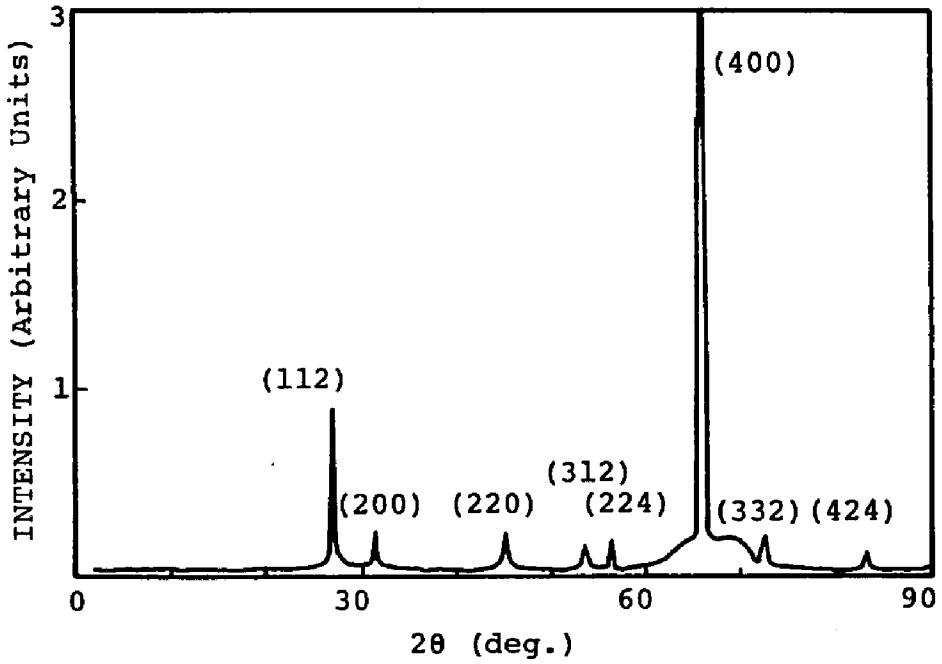

Figure 3.12 X-Ray Diffraction Spectrum of $ZnSnP_2$ Film Grown on (100) GaAs Substrate (Sample No. 78ZSP/GA)

Table 3.6 Comparisions of X-Ray Diffraction Spectra for $ZnSnP_2$ as Obtained from Calculations and from Measurements

Miller Index (hkl)*	Calculated				Measured	
	Zinc Blende Structure		Chalcopyrite Structure		Film on Quartz Subst.	
	Relative Intensity ($x10^6$)	I/I_{max}(%)	Relative Intensity ($x10^6$)	I/I_{max}(%)	Relative Intensity	I/I_{max}(%)
112 (111)	5.22	100.00	20.90	100.00	1663	100.00
200	1.07	20.60	2.87	13.74	220	13.23
220	2.95	57.33	3.94	18.85	545	32.77
312 (311)	2.20	42.10	5.87	28.09	515	30.97
224 (222)	0.26	4.98	1.05	5.02	106	6.37
400	0.45	8.71	1.21	5.80	99	5.95
332 (331)	0.84	16.13	1.12	5.36	124	7.46
420	0.31	5.93	0.50	2.39	61	3.67
424 (422)	0.94	18.00	1.25	5.98	127	7.67

* Miller Index in ( ) indicates the possible Index for Zinc Blende Structure.

(400) diffraction as shown in Figure 3.13. Diffraction peaks from the film grown on a GaAs substrate have the same pattern as the one from the film grown on a quartz substrate but with somewhat different relative intensity values. This may be due to the differences in the crystalline order in the two grown films.

The single crystal diffraction technique used here is useful for the structure identification but is not sensitive to small changes in lattice constant. Double crystal diffraction technique is required to distinguish (400) diffraction peak from $ZnSnP_2$ film from that of the (400) diffraction peak from the (100) GaAs substrate. Double crystal diffractometer, even though causes peak broadening for lattice constants which differ significantly from that of the analyzer, has good resolution for lattice constants close to that of the analyzer. Double crystal diffraction analysis on the grown films on GaAs substrates was not carried out in this work.

The Miller indices assigned to each of the observed diffraction peaks are presented in Figure 3.11 and in Figure 3.12. These assignments satisfy the general conditions of the I$\bar{4}$2d spacing group in which chalcopyrite $ZnSnP_2$ belongs [37,55]. The calculated lattice constant values from these measurements ranged from 5.64 Å to 5.67 Å which are in reasonable agreement with the reported value of 5.651 Å for the single crystal $ZnSnP_2$ platelets grown by solution

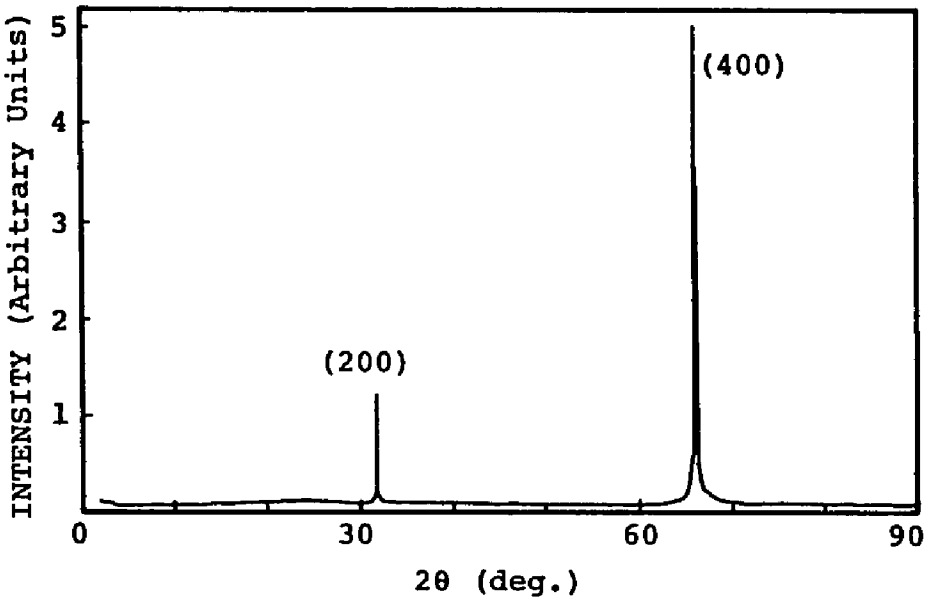

Figure 3.13 X-Ray Diffraction Spectrum of (100) GaAs Substrate

methods [1,37]. Small variations in the values of the lattice constants observed may be attributed to slight stoichiometric variations or to a presence of a phase mixture in the grown films.

3.6 Hall and Resistivity Measurements

Hall measurements were made on some of the films grown on semi-insulating GaAs substrates and on quartz substrates using the Van der Pauw technique [56] in the temperature range from 300°K to 625°K. All the films examined so far have p-type conductivity only. The room temperature Hall measurements showed the film resistivity of 0.1-10 Ω-cm and the carrier concentration in the range of 10^{16}-10^{18} cm^{-3}. The room temperature Hall mobility values were in the range of 35-47 cm^2/V-sec which are in good agreement with the reported values of 10-70 cm^2/V-sec [28].

High temperature Hall and resistivity measurements were made in the apparatus shown schematically in Figure 3.14. These measurements were carried out under the rough vacuum condition generated by a mechanical pump. A 9.0 KG magnetic field produced by an electromagnet with 4-inch pole piece was used for the measurements. The results of high temperature Hall and resistivity measurements on the sample No. 46ZSP/GA are plotted in Figure 3.15. In these experiments the temperature was increased from 300°K and measurements were made at 50°K interval.

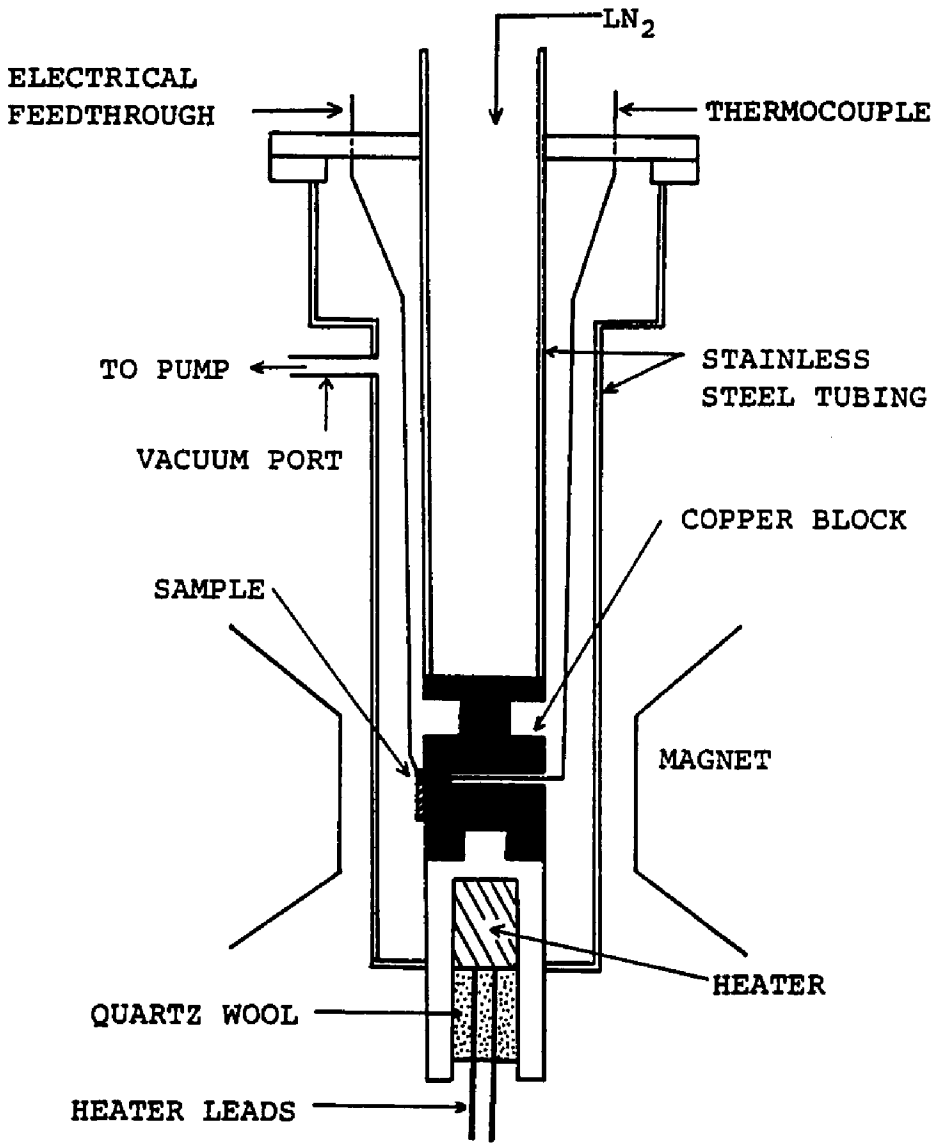

Figure 3.14 Schematic Diagram of Hall and Resistivity Measurement Apparatus

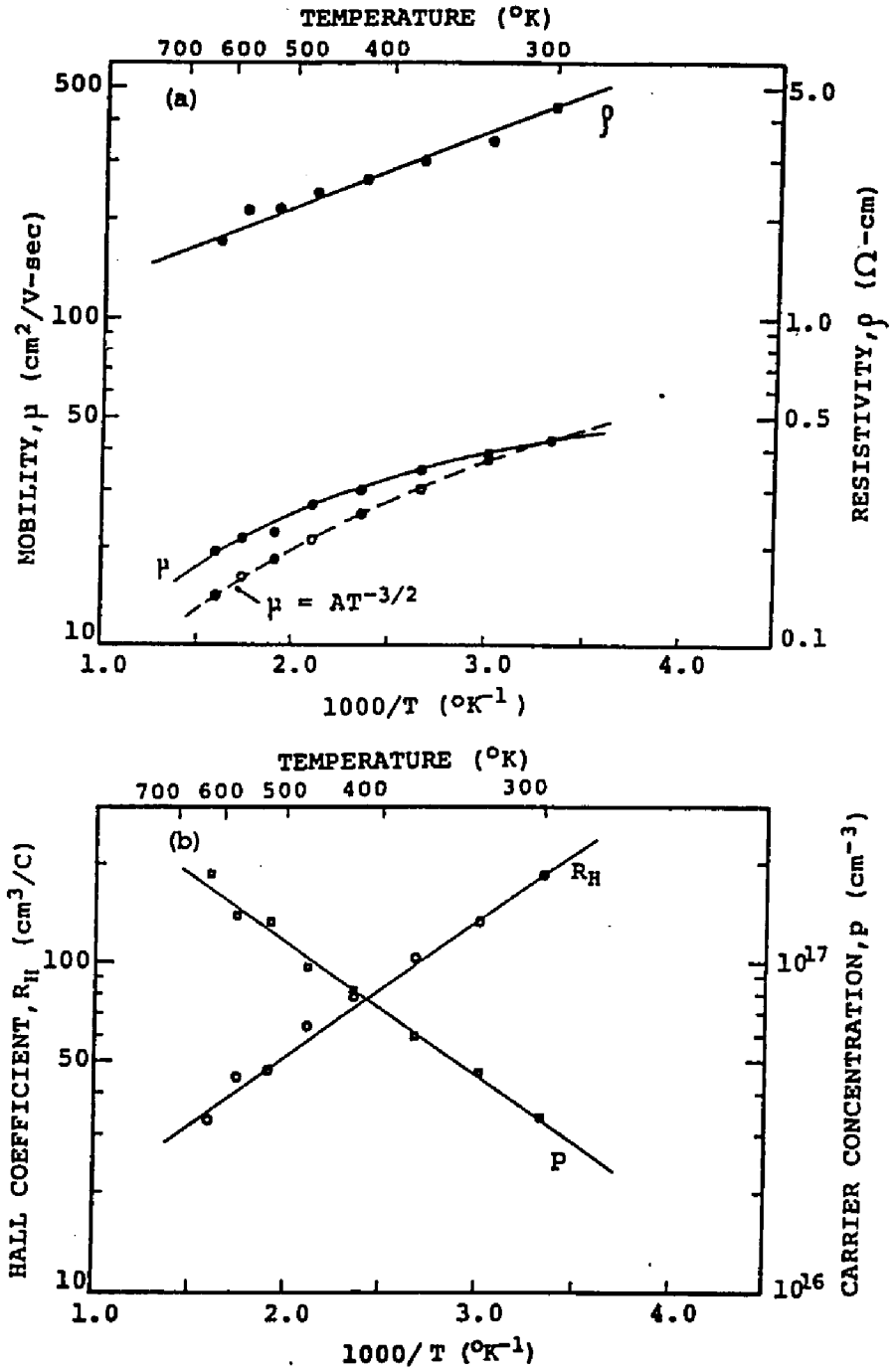

Figure 3.15 High Temperature Hall and Resistivity Measurement Results: (a)Resistivity and Mobility (b)Hall Coefficient and Carrier Concentration

As shown in Fig. 3.15(a) the mobility values deviated more from the line which is proportional to $T^{-3/2}$ as the temperature increased. Over the temperature range from 300°K to 626°K, the resistivity, ρ, shown in Figure 3.15(a) decreases as $\rho = \rho_o \exp(E/kT)$ where E = 0.046 eV. In the same temperature range, Hall coefficient, R_H, is positive indicating p-type conductivity. The temperature dependences of R_H and ρ are similar in the range of temperature where the measurements were made. The carrier concentration, p, is 3.37×10^{16} cm^{-3} at 300°K and increased to about 1.88×10^{17} cm^{-3} at 625°K. The activation energy for the acceptor level in the grown $ZnSnP_2$ film was calculated to be about 0.072 eV from the slope of carrier concentration vs. 1000/T line in Figure 3.15(b) [57]. The carrier concentration vs. 1000/T line over the temperature range from 300°K to 625°K is similar to the one observed in the ionization region.

Bulk resistivity of the film has been measured at 300°K and 77°K by placing vacuum evaporated and heat-treated In strip electrodes on two opposite ends of the film. These measurements showed a slight decrease of bulk resistivity at 77°K. Table 3.7 shows some of the results for the bulk resistivity measurements made at 300°K and 77°K.

3.7 Heterostructure Diodes

A heterostructure diode was formed between a near stoichiometric $ZnSnP_2$ film grown on n-type GaAs substrate.

Table 3.7 Bulk Resistivity Measurement Results at 300°K and 77°K on Some Samples.

Sample No.	Resistivity (Ω-cm) 300°K	77°K
42ZSP/GA	1.773	1.607
59ZSP/GA	0.266	0.224

In and Sn were used to make contacts to the $ZnSnP_2$ film and the GaAs substrate respectively. Figure 3.16 shows the I-V characteristics of the diode in the dark and under microscope light of intensity of 400 mW/cm^2. An open-circuit photovoltage of 0.3 V and a short-circuit current density of 15 $\mu A/cm^2$ have been obtained demonstrating a small photoresponse in this unoptimized structure. Heterostructure diodes with n-type In_2O_3 and p-type $ZnSnP_2$ have been reported with the best devices showing an open-circuit voltage of 0.3 V for 200 mW/cm^2 radiation at a photon energy of 1.97 eV [8]. The diodes fabricated in that work had been made from single crystal bulk material.

Some attempts have been made in this work to fabricate heterostructure diodes by growing $ZnSnP_2$ films on n-type CdS films deposited on SnO_2 coated glass substrates. The fabricated diodes showed no photoresponses.

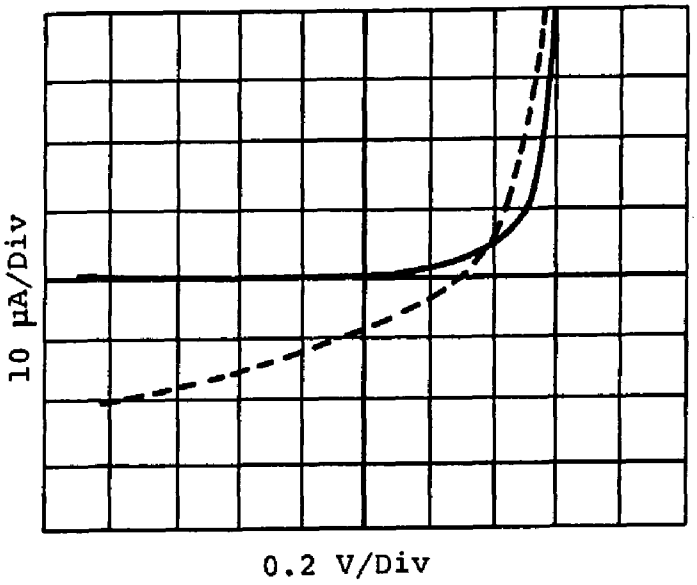

Figure 3.16 I-V Characteristics of Heterostructure Diode formed by p-type $ZnSnP_2$ Film on n-type GaAs Substrate (—— in the dark, - - - under Microscope Light)

CHAPTER 4

CONCLUSIONS

The objects of this study have been to obtain the optimized growth parameters for vacuum growth of thin films of $ZnSnP_2$ on GaAs substrate and on fused quartz substrate from three elemental sources and to characterize the grown films using different analytical techniques.

The major contributions of this research can be summerized as follows.

1. Thin films of a relatively little studied ternary semiconductor $ZnSnP_2$ have been grown for the first time by a vacuum growth technique somewhat similar to the MBE growth process. Elemental sources were used for the film growth on (100) GaAs and fused quartz substrates. The grown films were polycrystalline.

2. Quadrupole mass analyzer was used to solve the problem of decrease in Zn flux with time. This has been proved to be the most effective method on Zn flux control with less then ±2.5% flux variation from one run to the next as well as during a growth run.

3. The optimum growth parameters of 1.1×10^{-8} Torr for Zn flux as measured by the quadrupole probe, 1025°C for Sn source furnace temperature, 340°C for P source furnace temperature, and 280°C for substrate temperature have been

obtained. Critical ratio of Zn/Sn flux at the substrate has been estimated to be in the range of 3.5-4.7 for near stoichiometric film growth. Stoichiometric interval for the substrate temperature was determined to be in the range of 260-290°C.

4. SEM study with EDS analysis revealed that the film surface morphology was most sensitive to the Zn content in the grown film.

5. Optical transmission analysis showed that, without taking scattering effects at the film surfaces into account, the grown film has absorption coefficient, α, of greater than 10^5 cm^{-1} and direct bandgap of 1.62 eV which is very close to the generally accepted value of 1.66 eV for single crystal material.

6. X-Ray diffraction analysis showed that the grown films have chalcopyrite structure with lattice constant value in the range of 5.65-5.67 Å. It is evident from the analysis that there exists a preferred direction in $ZnSnP_2$ film growth on (100) GaAs substrate.

7. All the films tested showed only p-type conductivity with film resistivity values of 0.1-10 Ω-cm at the room temperature. Hall mobilities and carrier concentrations at the room temperature were in the range of 35-47 $cm^2/V\text{-}sec$ and 10^{16}-10^{18} cm^{-3} respectively.

8. The quality of films grown on GaAs substrates was

superior to that of films grown on quartz substrates.

9. Heterostructure diodes fabricated by growing $ZnSnP_2$ films on n-type GaAs substrates showed a small photoresponses, demonstrating the feasibility of photovoltaic applications of the grown film.

Recommandations for further research are as follows.

1. Sticking coefficient measurement of Zn molecules in the presence of Sn only and in the presences of Sn and P to help the understanding of the film growth mechanism.

2. Film growth using MBE system with *in situ* analysis instruments to identify and understand the initial film growth process on the substrate.

3. Search for the possibility of doping of the $ZnSnP_2$ film to change the conductivity from p-type to n-type to fabricate homojuction devices.

4. Growth of epitaxial layers on single crystal substrates to verify the possible device applications.

5. Study on appropriate contact material for the grown $ZnSnP_2$ films.

6. Fabrication of heterostructure devices for photovoltaic purposes.

REFERENCES

1. Shay, J. L. and J. H. Wernick, "Ternary Chalcopyrite Semiconductors: Growth, Electronic Properties, and Applications", Pergamon Press, New York, 1975.
2. Boudriot, H. and H. A. Schneider, "Application Possibilities of II-IV-V_2 Semiconductors in the Field of Optoelectronics", Act. Phys. Hung., Vol. 51, No. 4, 1981, pp. 361-370.
3. Podol'skii, V. V., I. A. Karpovich and B. N. Zvonkov, "Hall Mobility of Electrons in $CdSnP_2$ Single Crystals", Sov. Phys. Semicond., Vol. 10, No. 5, 1976, pp. 594-595.
4. Goryunova, N. A., E. I. Leonov, V. M. Orlov, A. F. Rodionov, V. I. Sokolova and V. P. Sondaevskii, "On Some Properties of $CdSnP_2$ in Strong Electric Field", Phys. Lett., Vol. 31A, No. 7, 1970, pp. 393-394.
5. Knight, S., E. Buehler and I. Camlibel, "Current Controlled Negative Resistance in $CdSnP_2$", J. Appl. Phys., Vol. 43, No. 8, 1972, pp. 3422-3424.
6. Prochukhan, V. D. and Yu. V. Rud, "Potential Practical Applications of II-IV-V_2 Semiconductors (review)" Sov. Phys. Semicond., Vol. 12, No. 2, 1977, pp. 121-135.
7. Shay, J. L., K. J. Bachman and E. Buehler, "Preparation and Properties of $CdSnP_2$/InP Heterojuctions Grown by LPE from Sn Solution", J. Appl. Phys., Vol. 45, No. 3,

1974, pp. 1302-1310.

8. Abdurachimov, A. A., Yu. V. Rud and V. M. Serginov, "Photoelectric Properties of Heterostructures in n-In_3O_2 - p-$ZnSnP_2$", Microelectronika, USSR, Vol. 12, No. 5, 1972, pp. 486-489.
9. Feigelson, R. S. and R. K. Route, "Vertical Bridgman Growth of $CdGeAs_2$ with Control of Interface Shape and Orientation", J. Cryst. Growth, Vol. 49, No. 2, 1980, pp. 261-273.
10. Shah, S. I. and J. E. Greene, "Growth and Physical Properties of $ZnGeAs_2$", Mat. Lett., Vol. 2, No. 2, 1983, pp. 115-118.
11. Valov, Yu. A., N. A. Goryunova, E. I. Leonov and V. M. Orlov, "Preparation and Properties of Ternary II-IV-V_2 Layers and Heterojunctions Based on Them", Act. Phys. Hung., Vol. 33, No. 1, 1973, pp. 1-15.
12. Siegel, W., G. Kuhnel, E. Ziegler, P. Kirsten and H. A. Schneider, "Orientation Dependance of Electrical and Optical Properties of $ZnSiP_2$ crystals Grown from Melt", Krist. Tech., Vol. 15, No. 8, 1980, pp. 947-954.
13. Miotkowski, I. and S. Miotkowski, "Solution Growth $CdGeP_2$ Crystals and Layers", J. Cryst. Growth, Vol. 50, No. 2, 1980, pp. 567-570.
14. Valov, Yu., Yu. V. Rud, F. N. Mukhtasi and R. V. Masaguto, "Growth of $ZnGeP_2$ Single-Crystals from Solution in a Thallium Melt", Inorg. Mater., Vol. 19,

No. 4, 1983, pp. 476-478.

15. Rubenstein, M. and R. W. Ure, Jr., "Preparation and Characteristics of $ZnSnP_2$", J. Phys. Chem. Solids, Vol. 29, 1968, pp. 551-555.

16. Winkler, K. and K. Hein, "Crystallization of $ZnSiP_2$ from Gas Phase", Krist. Tech., Vol. 12, No. 3, 1977, pp. 211-227.

17. Miotkowski, I., J. Weszka, J. Jurusik and S. Miotkowski, "Preparation of $CdGeP_2$ crystals by Chemical Vapor Transport", J. Cryst. Growth, Vol. 48, No. 3, 1980, pp. 479-482.

18. Avirovic, M., M. Lux-Steiner, N. Elrod, J. Honigschmid and E. Bucher, "Single Crystal Growth of $CdSiAs_2$ by Chemical Vapor Transort; Its Structure and Electrical Properties", J. Cryst. Growth, Vol. 67, No. 2, 1984, pp. 185-194.

19. Andrews, J. E., M. A. Littlejohn, G. A. Igwa and R. T. Pickett, "MOCVD growth and Characterization of $ZnSiAs_2$", J. Cryst. Growth, Vol. 56, No. 1, 1982, pp. 1-6.

20. Andrews, J. E., H. H. Stadelmaier, M. A. Littlejohn and J. Comas, "Vapor-Phase Epitaxial Growth of $ZnSiAs_2$ on Ge and GaAs Substrates", J. Electrochem. Soc., Vol. 128, No. 7, 1981, pp. 1563-1568.

21. Sansregret, Joseph, "The Growth of Thin Films of Zinc Tin Phosphide", Mat. Res. Bull., Vol. 16, No. 5, 1981,

pp. 607-611.

22. Sansregret, Joseph L., "Method for Depositing Photoconductive Zinc Tin Phosphide", U.S. Patent No. 4,311,728., Publ., Jan. 19, 1982.

23. Samaan, A. N., (private communications), Solar Energy Research Institute, 1987.

24. Bachman, K. J., E. Buehler, J. L. Shay and G. W. Kammlott, "The Preparation of $CdSnP_2$/InP Heterojunctions by Liquid Phase Epitaxy from Sn-solutuin", J. Elec. Mat., Vol. 3, No. 2, 1974, pp. 451-473.

25. Trifonova, E. P. and A. S. Popov, "n-n Heterojunctions $CdSnP_2$-InP", Phys. Stat. Solids (a), Vol. 38, 1976, pp. 37-40.

26. Danilov, V. I. and I. A. Karpovic, "Preparation of $CdSnAs_2$ Films by Means of Liquid Phase Epitaxy", Inorg. Mater., Vol. 17, No. 1, 1981, pp. 7-9.

27. Takenoshita, H. and T. Nakau, "LPE Growth of $ZnSnAs_2$ on a ZnSe Substrate from a Sn Solution", Japan. J. Appl. Phys. 2, Vol. 21, No. 4, 1982, pp. 212-214.

28. Davis, G. A. and C. M. Wolfe, "Liquid Phase Epitaxial Growth of $ZnSnP_2$ on GaAs", J. Electrochem. Soc., Vol. 130, No. 6, 1983, pp. 1408-1412.

29. Bedair, S. M. and M. A. Littlejohn, "Liquid Phase Epitaxy of II-IV-V_2 Chalcopyrite Compounds", J. Electrochem. Soc., Vol. 125, No. 6, 1978, pp. 952-956.

30. White, F. R., A. H. Clark, M. C. Graf, S. P. Grindle and L. L. Kazmerski, "Growth of $CuInSe_2$ Films using Molecular Beam Epitaxy", J. Vac. Sci. Technol., Vol. 16, No. 2, 1979, pp. 287-289.

31. Grindle, S. P., A. H. Clark, S. Rezaie-Serej, E. Falconer, J. McNeily and L. L. Kazmerski, "Growth of $CuInSe_2$ by molecular beam epitaxy", J. Appl. Phys., Vol. 51, No. 10, 1980, pp. 5464-5469.

32. Samaan, A. N., R. Vaidhyanathan, R. Noufi and R. D. Tomlinson, "Growth and Characterization of Polycrystalline $CuInSe_2$ Thin Films", Solar Cells, Vol. 16, 1986, pp. 181-198.

33. Burton, L. C. and L. H. Slack, "$CdSiAs_2$ Thin Films for Solar Cell Applications", DOE Document No. DOE/ET/23007-2, 1979.

34. Shah, S. I. and J. E. Greene, "Growth and Physical Properties of Amorphous and Single Crystal $ZnGeAs_2$ Layers Deposited on (100) GaAs by Sputtering Deposition in Excess Zn and As_4", J. Cryst. Growth, Vol. 68, No. 2, 1984, pp. 537-544.

35. Wolfe, C. M., G. A. Davis and S. J. Hsieh, "Epitaxial Growth of $CdSnP_2$", Gov. Document No. AD-A090285, 1980.

36. Zamanian, B., "Growth and Characterization of Vacuum Deposited Films of $ZnSnP_2$", Master Thesis, Louisiana State University, 1984.

37. Vaipolin, A. A., N. A. Goryunova, L. I. Kleshchinskii,

G. V. Loshakova and E. O. Osmanov, "The Structure and Properties of the Semiconducting Compound $ZnSnP_2$", Phys. Stat. Sol., Vol. 29, 1968, pp. 435-442.

38. Sze, S. M., "Physics of Semiconductor Devices", John Wiley, N.Y., 1981, pp. 797-798.

39. Sun, L. Y., L. L. Kazmerski, A. H. Clark, P. J. Ireland and D. W. Morton, "Absorption Coefficient Measurements for Vacuum-deposited Cu-ternary Thin Films", J. Vac. Sci. Technol., Vol. 15, No. 2, 1978, pp. 265-268.

40. Chaney, D. C., "A Molecular Beam Epitaxy System for the Growth of Semiconductor Materials", M.S. Thesis, University of Notre Dame, 1980.

41. Nesmeyanov, A. N., "Vapor Pressure of the Chemical Elements", N.Y. Academic Press, 1963.

42. Cho, A. Y. and J. R. Arthur, "Molecular Beam Epitaxy", Prog. Solid State Chem., Vol. 10, 1975, pp. 157-191.

43. Joyce, B. A. and C. T. Foxon, "Growth and Doping of Semiconductor Films by Molecular Beam Epitaxy", Inst. Phys. Conf. Ser., No. 32, 1977, pp. 17-37.

44. Arthur, J. R., "Adsorption of Zn on GaAs", Surf. Sci., Vol. 38, 1973, pp. 394-412.

45. Smith, D. L., "Epitaxial Zn_3P_2 Film Grown by Activated Vacuum Evaporation of the Elements", Final Report on SERI subcontract No. XS-9-8041-7, 1981.

46. Reif, F., "Fundamentals of Statistical and Thermal Physics", McGraw-Hill, New York, 1965, pp. 461-471.

47. Myers, T. H. and J. F. Schetzina, "Molecular Beam Source for High Vapor Pressure Materials", J. Vac. Sci. Technol., Vol. 20, 1982, pp. 134-136.

48. Maissel, Leon I. and Reinhard Glang (Eds.), "Handbook of Thin Film Technology', Eds., McGraw Hill, New York, 1970.

49. Jackson, S. C., "Engineering Analysis of the Deposition of Cadmium-Zinc Sulfide Semiconductor Film", Ph.D. Dissertation, University of Delaware, 1984.

50. Schwartz, B. and J. C. Sarace, "Low-Temperature Alloy Contacts to Gallium Arsenide Using Metal Halide Fluxes", Solid State Electronics, Vol. 9, 1966, pp. 859-864.

51. Ghandhi, Sorab K., "VLSI Fabrication Principles: Silicon and Gallium Arsenide", John Wiley & Sons, N.Y., 1983, pp. 452.

52. Abdurakhimov, A. A., L. V. Kradinova, Z. A. Parimbekov and Yu. V. Rud, "Schottky diodes made of p-type $ZnSnP_2$", Sov. Phys. Semicond., Vol. 16, No. 2, 1982, pp. 156-159.

53. Cho, A. Y., "Impurity profiles of GaAs epitaxial layers doped with Sn, Si, and Ge grown with molecular beam epitaxy", J. Appl. Phys., Vol. 46, No. 4, 1975, pp. 1733-1735.

54. Mott, N. F. and E. A. Davis, "Electronic Processes in Non-crystalline Materials", 2nd Eds., Clarendon Press,

Oxford, England, 1979, pp. 272-274.

55. International Union of Crystallography, "International Tables for X-Ray Crystallography, Volume 1: Symmetry Groups", Kynoch Press, Birmingham, England, 1952.

56. ANSI/ASTM F76-73, "Standard Method for Measuring Hall Mobility and Hall Coefficient in Extrinsic Semiconductor Single Crystals", Annual Book of ASTM Standards, 1976, pp. 1-17.

57. Smith, R. A., "Semiconductors", Cambridge University Press, England, 1968, pp. 82-92.

58. International Union of Crystallography, "International Tables for X-Ray Crystallography, Volume 4: Revised and Supplementary Tables", Kynoch Press, Birmingham, England, 1974.

59. Cullity, B. D., "Elements of X-Ray Diffraction", 2nd Ed. Addison-Wesley, Massachusetts, 1978.

APPENDIX

CALCULATION OF X-RAY DIFFRACTION INTENSITIES FOR $ZnSnP_2$

The theory applied to identify the structure of a material from its X-ray diffraction spectrum utilizes the fact that positions of the atoms within an unit cell affect the intensity but not the direction of the diffracted X-ray beam. Hence, the atomic positions in the unit cell can be determined by observing the intensities of the diffracted X-ray beam while the unit cell can be determined by observing the directions of the diffracted X-Ray bean.

Two assumptions are made in calculating the expected relative intensities of the X-ray diffractions from the single crystal chalcopyrite $ZnSnP_2$ and from the Zinc Blende $ZnSnP_2$ structure. These assumptions are given below.

1. All unit cells consist of not ions but atoms only. Therefore, f_P, f_{Zn}, and f_{Sn} are atomic scattering factors for the P, Zn, and Sn atoms respectively.

2. For Zinc Blende structure $ZnSnP_2$, Zn and Sn atoms have random distributions among the accessible anion lattice sites.

The structure factor describes how the atomic arrangement given by *uvw* for each atom in the unit cell affects the scattered X-ray beam. If a unit cell contains atoms 1, 2, 3, ..., N, with fractional coordinates $u_1v_1w_1$, $u_2v_2w_2$, ..., $u_Nv_Nw_N$ and atomic scattering factors f_1, f_2,

..., f_N, then the structure factor for a unit cell, F_{hkl}, for the *hkl* reflection is given by

$$F_{hkl} = \sum^{N} f_n e^{2\pi i(hUn+kVn+lWn)} \qquad (A.1)$$

where N is the number of atoms in the unit cell, f_n is atomic scattering factor, and (Un, Vn, Wn) is the location of the nth atom in the unit cell. The location of the atoms are at $(Un, Vn, Wn) = (x/a, y/b, z/c)$ where a, b, and c are crystal axes.

The intensity of the X-ray beam diffracted by the unit cell of N atoms from (*hkl*) plane is proportional to $|F_{hkl}|^2$ without considering structure multiplicity factor, p, and Lorentz factor, $[(1+\cos^2 2\theta)/\sin^2\theta\cos\theta]$. The relative intensities of the X-ray beam diffracted from (*hkl*) plane, therefore, can be expressed as

$$I_{Rel.} = |F_{hkl}|^2 p[(1+\cos^2 2\theta)/\sin^2\theta\cos\theta] \qquad (A.2)$$

Chalcopyrite $ZnSnP_2$ has a tetragonal structure with $c/a = 2$ and $\alpha=\beta=\gamma= 90°$. If Zn and Sn atoms are equally and randomly distributed in the unit cell, $ZnSnP_2$ will have a Zinc Blende structure. In this case, the unit cell is a cube with a = b = c. Then the locations of Zn, Sn, and P atoms are as follows.

Zn and Sn atoms:	0 0 0,	1/2 1/2 0,
	1/2 0 1/2,	0 1/2 1/2,

P atoms: 1/4 1/4 1/4, 3/4 3/4 1/4,
3/4 1/4 3/4, 1/4 3/4 3/4.

Then, the structure factor F_{hkl} for Zinc Blende $ZnSnP_2$ becomes

$$F_{hkl} = [(f_{Zn}+f_{Sn})/2][e^{2\pi i(0)}+e^{2\pi i(h/2+k/2)} +e^{2\pi i(k/2+l/2)}+e^{2\pi i(h/2+l/2)}] +f_p[e^{2\pi i(h/4+k/4+l/4)}+e^{2\pi i(3h/4+3k/4+l/4)} +e^{2\pi i(3h/4+k/4+3l/4)}+e^{2\pi i(h/4+3k/4+3l/4)}] \quad (A.3)$$

After simple manipulations, equation (A.3) becomes

$$F_{hkl} = \{[(f_{Zn}+f_{Sn})/2]+f_p e^{\pi i(h+k+l)/2}\} [1+e^{\pi i(h+k)}+e^{\pi i(k+l)}+e^{\pi i(h+l)}] \quad (A.4)$$

Diffraction peaks occurs when the above expression has non-zero maximum values. For this condition, $h+k$, $k+l$, and $h+l$ must be even. Therefore, h, k, and l should be all even or all odd and the mixed modes are not allowed for diffraction peaks. Then, equation (A.4) can be written as

$$F_{hkl} = 4\{[(f_{Zn}+f_{Sn})/2]+f_p e^{2\pi i(h+k+l)/2}\} \quad (A.5)$$

and

$$|F_{hkl}|^2 = 16\{[(f_{Zn}+f_{Sn})/2]^2+f_p^2 +(f_{Zn}+f_{Sn})f_p\cos[\pi(h+k+l)/2]\} \quad (A.6)$$

Atomic scattering factors for Zn, Sn , and P atoms are shown in Fig. A.1 plotted from the table of atomic

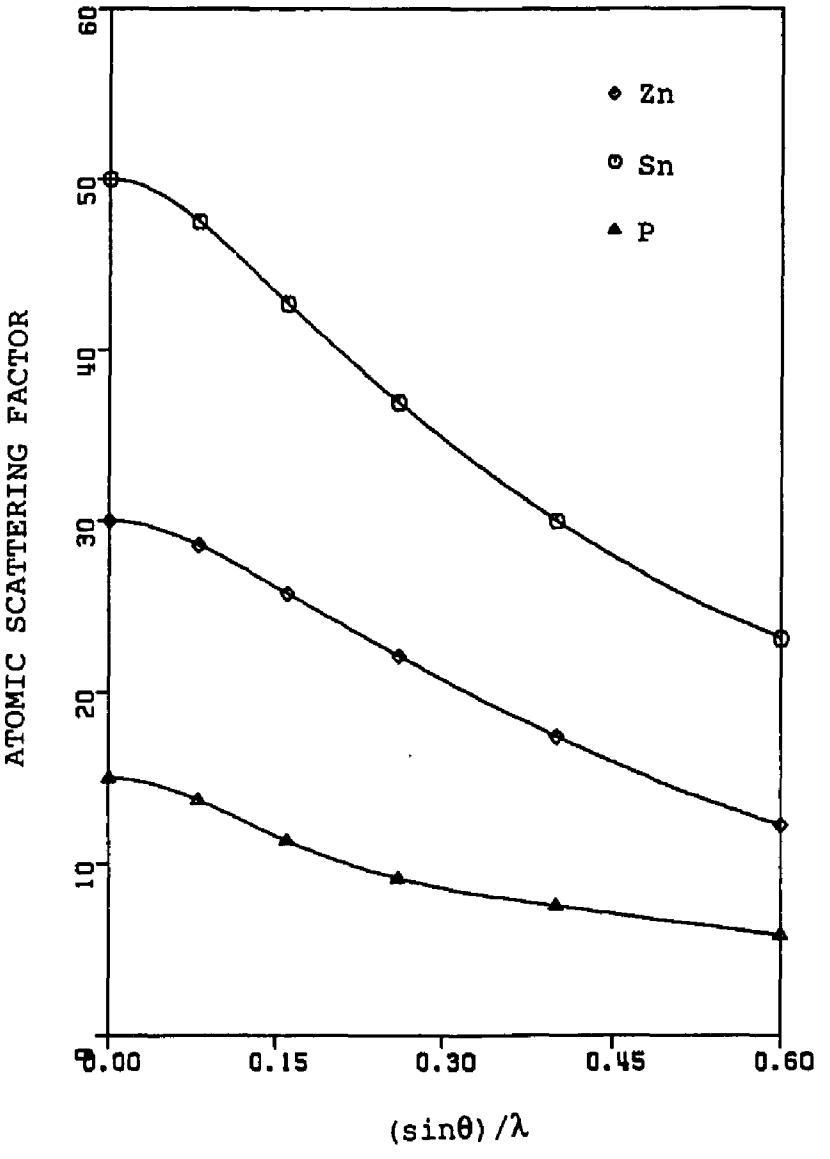

Figure A.1 Plot of Atomic Scattering Factors for Zn, Sn, and P Atoms

scattering factors for X-ray diffraction [58]. The parameter $(\sin\theta)/\lambda$ for a given *hkl* can be determined from

$$d_{hkl} = n\lambda/2\sin\theta = a/(h^2+k^2+l^2)^{1/2} . \qquad (A.7)$$

The structure multiplicity factor, p, for the X-ray powder diffraction for various crystal structures are already available [59].

From equations (A.2), (A.6), and (A.7), theoretical relative intensities of the diffracted X-ray beams for Zinc Blende structure $ZnSnP_2$ can be obtained.

For the chalcopyrite structure $ZnSnP_2$ with c = 2a, the locations of Zn, Sn, and P atoms are as follows.

Zn atoms:	0 0 0,	1/2 0 1/4,
	1/2 1/2 1/2,	0 1/2 3/4.
Sn atoms:	1/2 1/2 0,	0 1/2 1/4,
	0 0 1/2,	1/2 0 3/4.
P atoms:	1/4 1/4 1/8,	1/4 1/4 5/8,
	1/4 3/4 3/8,	1/4 3/4 7/8,
	3/4 1/4 3/8,	3/4 1/4 7/8,
	3/4 3/4 1/8,	3/4 3/4 5/8.

By following the same procedures as in the calculations of the relative intensities of the diffracted X-ray beams for the Zinc Blende structure $ZnSnP_2$ with the parameter $(\sin\theta)/\lambda$ determined from

$$d_{hkl} = n\lambda/2\sin\theta = a/[h^2+k^2+(1/2)^2]^{1/2} \qquad (A.8)$$

for a given *hkl*, theoretical intensities of the diffracted X-ray beams for chalcopyrite structure $ZnSnP_2$ can be calculated.

Table A.1 and A.2 show the calculated relative intensities of the diffracted X-ray beams for Zinc Blende $ZnSnP_2$ and chalcopyrite $ZnSnP_2$ respectively. The relative intensities of the diffracted X-ray beams obtained from measurement for the thin films of $ZnSnP_2$ grown on quartz substrate is given in Table A.3. In these tables, the ratio of intensity to the maximum intensity, I/I_{max}, is more important for the structure identification. From these tables, it can be concluded that the grown $ZnSnP_2$ film has the chalcopyrite structure with the presence of a possible phase mixture.

Table A.1 Calculated Relative Intensities of the Diffracted X-Ray Beam for Zinc Blende Structure $ZnSnP_2$ for Cu K_α Radiation

Miller Index (hkl)	$\sin\theta/\lambda$	2θ	f_{Zn}	f_{Sn}	f_P	p	Calculated Relative Intensity ($\times 10^6$)	I/I_{max}(%)
111	0.153	27.33	24.40	42.38	11.07	8	5.22	100.00
200	0.177	31.666	23.35	40.85	10.52	6	1.07	20.60
220	0.250	45.393	20.45	36.50	9.15	12	2.95	57.33
311	0.293	53.80	18.86	34.15	8.53	24	2.20	42.10
222	0.3065	56.402	18.41	33.44	8.36	8	0.26	4.98
400	0.354	66.14	17.05	30.99	7.85	6	0.45	8.71
331	0.3857	72.973	16.18	29.32	7.55	24	0.84	16.13
420	0.3957	75.191	15.91	28.90	7.48	24	0.31	5.93
422	0.4335	83.874	15.02	27.43	7.13	24	0.94	18.00

Table A.2 Calculated Relative Intensities of the Diffracted X-Ray Beam for Chalcopyrite Structure $ZnSnP_2$ for Cu K_α Radiation

Miller Index (hkl)	$\sin\theta/\lambda$	2θ	f_{Zn}	f_{Sn}	f_P	p	Calculated Relative Intensity ($\times 10^6$)	I/I_{max}(%)
112	0.153	27.33	24.40	42.38	11.07	8	20.90	100.00
200	0.177	31.666	23.35	40.85	10.52	4	2.87	13.74
220	0.250	45.393	20.45	36.50	9.15	4	3.94	18.85
312	0.293	53.80	18.86	34.15	8.53	16	5.87	28.09
224	0.3065	56.402	18.41	33.44	8.36	8	1.05	5.02
400	0.354	66.14	17.05	30.99	7.85	4	1.21	5.80
332	0.3857	72.973	16.18	29.32	7.55	8	1.12	5.36
420	0.3957	75.191	15.91	28.90	7.48	8	0.50	2.39
424	0.4335	83.874	15.02	27.43	7.13	8	1.25	5.98

Table A.3 Measured Relative Intensities of the Diffracted X-Ray Beam from $ZnSnP_2$ Film grown on Quartz Substrate (Sample No. 90ZSP/CQ)

Miller Index (hkl)	Measurement	
	Relative Intensity (a.u)	I/I_{max} (%)
112	1663	100.00
200	220	13.23
220	545	32.77
312	515	30.97
224	106	6.37
400	99	5.95
332	124	7.46
420	61	3.67
424	127	7.67

VITA

Hyun Yong Shin was born in Chollabukdo, Korea on June 10, 1952. He received his Bachelor's and Master's degrees in Electrical Engineering from Yonsei University, Seoul, Korea, in 1979 and 1981, respectively. Since August 1981, he has been pursuing further graduate studies at Louisiana State University, Baton Rouge, where he has worked as a teaching assistant and as a research assistant in the Electrical and Computer Engineering Department. He has been an Honor Student and a recipient of the Honor Student Scholarship (1976-78). He is a student member of Institute of Electrical and Electronics Engineering.

He is presently a candidate for the degree of Doctor of Philosophy in Electrical Engineering.

DOCTORAL EXAMINATION AND DISSERTATION REPORT

Candidate: Hyun Yong Shin

Major Field: Electrical Engineering

Title of Dissertation: Vacuum Growth and Characterization of Thin Films of Zinc Tin Diphosphide

Approved:

P. K. Ajmera
Major Professor and Chairman

Dean of the Graduate School

EXAMINING COMMITTEE:

Date of Examination:

June 11, 1987